A Unified Force Density Framework for Plasma Confinement: Integrating Navier-Stokes with Local Interaction Field Equilibrium (LIFE)

Wim Vegt
Physicist & Researcher (Ret.)
Eindhoven
(Formerly TU/e)

Abstract

Achieving stable magnetic confinement in nuclear fusion plasmas remains a profound theoretical and engineering challenge. Fundamentally, plasma confinement is a problem of macroscopic force density equilibrium. However, standard Magnetohydrodynamic (MHD) models treat mechanical fluid dynamics and electrodynamics as coupled but distinct systems, often relying on fragmented approximations that struggle to predict complex plasma instabilities.

This paper introduces a unified theoretical framework that seamlessly integrates the mechanical fluid dynamics of the Navier-Stokes equations (governing mechanical pressure and fluid velocity) with the Local Interaction Field Equilibrium (LIFE) theory. By strictly expressing all physical interactions—including mechanical pressure, radiation pressure, electromagnetic field tensors, inertia, and gravitational coupling—in identical dimensions of force density (N/m^3), we derive a single, continuous equilibrium field equation.

This exact dimensional consistency eliminates the mathematical boundaries between the material plasma (Deuterium infusion) and the energetic confinement fields (microwave heating and magnetic containment). The resulting unified N/m^3 equation provides a novel, rigorous analytical foundation for understanding high-energy plasma dynamics, offering new predictive pathways for mitigating instabilities in Tokamak and stellarator confinement systems.

Keywords:

Magnetohydrodynamics (MHD), Plasma Confinement, Force Density Equilibrium, Navier-Stokes Equations, Macroscopic Plasma Stability, Electrodynamic Fluid Interactions

1. Energy Confinement Dynamics in Ultra-Dense, High-Temperature Plasmas

In both classical mechanics and electrodynamics, the most stable mechanism for high-capacity energy storage within a bounded spatial configuration is the excitation of resonant standing waves, or eigenmodes. Just as one-dimensional mechanical energy is conserved within the resonant harmonics of a vibrating string, three-dimensional electromagnetic energy can be stably confined within localized solitonic wave packets (e.g., GEONs) when driven at specific resonant eigenfrequencies.

The fundamental challenge in achieving viable nuclear fusion lies in the stable macroscopic confinement of immense kinetic and radiation energy densities within an ultra-dense, high-temperature plasma. Conventional Tokamak confinement strategies, which predominantly attempt to maintain continuous, quasi-laminar plasma flows along the azimuthal (toroidal) axis, are inherently susceptible to macroscopic instabilities. Forcing a purely directional flow limits the energy-carrying capacity of the plasma and inevitably leads to turbulent breakdown.

To achieve absolute macroscopic stability and prevent material degradation of the confinement vessel, the plasma must not merely flow; it must be structured as a three-dimensional resonant cavity. In this proposed topological confinement model, the immense kinetic and radiative energy is stored via macroscopic toroidal standing waves. Because the kinetic temperature of a plasma is directly proportional to the square of its particle velocity $\left(T \propto \left\langle v^2 \right\rangle\right)$, thermal management can be actively controlled through specific boundary conditions.

Radially, this necessitates the formation of a **velocity anti-node** at the geometric centre of the toroidal cross-section (the magnetic axis), ensuring that the maximum particle velocity—and therefore the extreme peak temperatures required for fusion—remains tightly concentrated at the core. Conversely, the wave topology must dictate a **velocity node** at the outer confinement boundaries. By forcing the macroscopic velocity amplitude (and consequently the kinetic temperature) to a minimum at the inner surface of the Tokamak, the physical structure is inherently protected from catastrophic thermal loads.

Furthermore, to satisfy continuous boundary conditions and prevent destructive interaction, the azimuthal (toroidal) circumference of the confinement field must perfectly match an exact integer multiple of the fundamental wavelength of the confined plasma. This establishes a stable, closed-loop, three-dimensional geometric resonance.

The mathematical formulation required to describe and sustain this three-dimensional plasma resonance cannot be derived from standard, disjointed Magnetohydrodynamic (MHD) models. Instead, it necessitates a strict synthesis of

mechanical fluid dynamics and electromagnetic equilibrium. This is achieved by unifying the compressible Navier-Stokes equations with the Intrinsic Equilibrium Equation derived from Local Interaction Field Equilibrium (LIFE) theory. By rigorously expressing all constituent mechanical, thermal, and electromagnetic field interactions in identical dimensions of volumetric force density (N/m^3), we derive a singular, continuous field equation capable of governing the 3D resonant confinement of ultra-dense fusion plasmas.

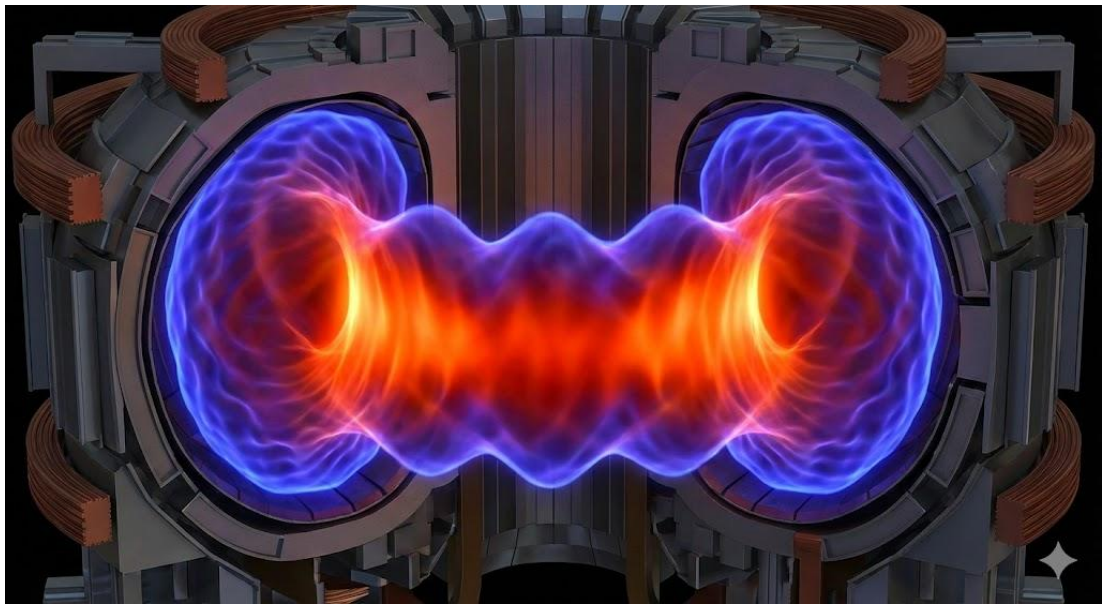

Figure 1: Conceptual visualization of a Tokamak operating as a macroscopic three-dimensional resonant cavity. The fusion plasma is structured as a toroidal standing wave, demonstrating active thermal management through localized boundary conditions. A **velocity anti-node** (region of maximum kinetic temperature, visible as the bright, high-energy core) is maintained at the central magnetic axis to sustain optimal fusion conditions. Simultaneously, a **velocity node** (region of minimum kinetic temperature, visible as the cooler boundary) is strictly enforced at the inner surface of the Tokamak, inherently shielding the physical confinement vessel from catastrophic thermal degradation.

2. Local Interaction Field Equilibrium (LIFE) and Generalized Acceleration

In the highly turbulent environment of an ultra-dense, high-temperature fusion plasma, macroscopic stability is fundamentally governed by the continuous interplay of diverse volumetric force densities. Among these, the acceleration force densities—arising from the complex kinetic motion of the fluid and its interaction with external fields—play a critical role in dictating the overall confinement efficacy.

Standard Magnetohydrodynamic (MHD) models often treat gravitational forces and electromagnetically induced kinetic accelerations as distinct, compartmentalized phenomena. However, within the framework of Local Interaction Field Equilibrium (LIFE), this theoretical boundary is mathematically dissolved.

The LIFE framework introduces a generalized equivalence principle directly applicable to plasma fluid dynamics. Within this continuous field model, there is no dimensional or physical distinction between the ambient gravitational acceleration induced by Earth's mass and the severe radial and azimuthal (toroidal) accelerations imposed by the Tokamak's primary magnetic fields and its toroidal geometry.

By unifying these kinematic and gravitational effects into a single, comprehensive acceleration force density tensor (strictly expressed in N/m^3), the LIFE theory ensures that all spatial accelerations acting upon the plasma are treated with absolute mathematical equivalence. This unified approach provides a superior analytical foundation for modelling the complex, non-inertial forces that drive turbulent instabilities within toroidal confinement systems.

The Einstein field equations (EFE), commonly referred to as Einstein's equations, establish a profound connection between the geometry of spacetime and the distribution of matter contained within it. Einstein (2014) [36] More precisely, the EFE articulate the relationship between the geometrical attributes of spacetime and the distribution of mass-energy, momentum, and stress. These equations consequently dictate the metric tensor of spacetime corresponding to a specified configuration of stress-energy-momentum within the spacetime continuum.

The fundamental principle underlying General Relativity (Sciama D. W. 1964) [16] is predicated upon a curved four-dimensional spacetime continuum. Similarly, the foundational concept inherent in this groundbreaking theory is articulated through a four-dimensional universal equilibrium, as delineated in equation (6).

$$G_{\mu\nu} + \Lambda\, g_{\mu\nu} = \kappa\, T_{\mu\nu} \qquad (1)$$

In which $G_{\mu\nu}$ equals the Einstein Tensor, $g_{\mu\nu}$ equals the Metric Tensor, $T_{\mu\nu}$ equals the Stress-Energy tensor, Λ equals the cosmological constant and κ equals the Einstein gravitational constant.

The core principle underlying General Relativity pertains to a curved 4-dimensional Space-Time Continuum. Similarly, the fundamental concept in this novel theory revolves around a 4-dimensional Universal Equilibrium delineated by equation (6).

Central to this novel theory is the vectorial summation of force densities denoted in [N/m^3]. Force densities hold universal significance and are interchangeable irrespective of their source. Vegt Wim (1995) [3] Within this framework, fields solely engage with analogous fields. The theory contemplates three distinct categories of physical fields: Electric Fields, Magnetic Fields, and Gravitational Fields.

The outcome of the interaction between two corresponding fields manifests as a force density articulated in [N/m^3]. When two electric fields interact, the resultant force density is an electric force density delineated in [N/m^3]. Similarly, the convergence of two magnetic fields yields a magnetic force density expressed in [N/m^3]. Likewise, the intersection of two gravitational fields produces a gravitational force density expressed in [N/m^3]. At the core of this theory lies the foundational principle that all force densities collectively establish a universal equilibrium. This elucidation can be found in Reference (Vegt W. 2022)[11], specifically detailed within equations (4) through (22).

The vectorial force densities are obtained from the divergence of the sum of the Electromagnetic Stress-Energy tensor $\overline{\overline{T}}$ and the newly introduced Gravitational Tensor $\overline{\overline{J}}$.

$$\kappa\, T_{\mu\nu} \;\Leftrightarrow\; T_{\mu\nu} \;+\; J_{\mu\nu} \tag{2}$$

Equation (2) encompasses the sum of the Energy Stress Tensor $T_{\mu\nu}$ which includes the terms that characterize the vector components of the electric field intensity $\left(\overline{E_x}, \overline{E_y}, \overline{E_y}\right)$, as well as the vector components of the magnetic field intensity $\left(\overline{H_x}, \overline{H_y}, \overline{H_y}\right)$. Additionally, it incorporates the Gravitational Tensor $J_{\mu\nu}$, which accounts for the terms that describe the vector components of the gravitational field intensity $\left(\overline{g_x}, \overline{g_y}, \overline{g_y}\right)$.

$T_{\mu\nu}$

The stress–energy tensor describes the density and flux of electromagnetic energy and momentum in space-time, generalizing the stress tensor of Newtonian physics. It is an attribute of matter, radiation and non- gravitational force fields.

The Gravitational Tensor $J_{\mu\nu}$ describes the density and flux of gravitational energy and momentum in space-time. It is an attribute of gravitational energy density and non- electromagnetic force fields.

The 4-dimensional divergence of the sum of the Electromagnetic Stress-Energy tensor and the Gravitational Tensor expresses the 4-dimensional Force-Density vector (expressed in $[N/m^3]$ in the 3 spatial coordinates) as the result of Electro-Magnetic-Gravitational interaction.

$$f^{\mu} = \partial_{\nu} \left(T^{\mu\nu} + J^{\mu\nu} \right) \tag{3}$$

In vector notation the 4-dimensional Force-Density vector can be written as:

$$\overline{f}^{4} = \begin{pmatrix} f_4 \\ f_3 \\ f_2 \\ f_1 \end{pmatrix} = \Box \bullet \left(\overline{\overline{T}} + \overline{\overline{J}} \right) \tag{4}$$

Analogous to the three-dimensional vector operator known as Nabla $(\nabla \cdot)$ which signifies the three-dimensional divergence within a vector space, the vector operator $(\Box \cdot)$ denotes the four-dimensional divergence within the Minkowski spacetime of four dimensions. Vegt Wim (2024) [42]

The essential boundary condition for this alternative gravitational approach is that the Force 4-vector must be zero across all four dimensions, thereby signifying a universal four-dimensional equilibrium. Vegt Wim (1995) [3] and Kaye Joel (April 2014) [35]

The divergence of the stress-energy tensor $T_{\mu\nu}$ signifies the electromagnetic force densities arising from electromagnetic fields. Specifically, the divergence of the stress-energy tensor, which denotes the resultant force density of an electromagnetic field acting upon itself, is equal to zero. In contrast, the divergence of the stress-energy tensor that reflects the resultant force density between two distinct electromagnetic fields typically does not equate to zero.

The divergence of the gravitational tensor $J_{\mu\nu}$ signifies the gravitational force densities arising from gravitational fields. Specifically, the divergence

of the gravitational tensor, which denotes the resultant force density of a gravitational field acting upon itself, is equal to zero. In contrast, the divergence of the gravitational tensor that reflects the resultant force density between two distinct gravitational fields typically does not equate to zero.

$$\bar{\bar{f}}^4 = \begin{pmatrix} f_4 \\ f_3 \\ f_2 \\ f_1 \end{pmatrix} = \square \bullet \left(\bar{\bar{\mathrm{T}}} + \bar{\bar{\mathrm{J}}} \right) = \bar{0}^4 \tag{5}$$

Within this innovative framework, the interactions among electric-electric fields, magnetic-magnetic fields, and gravitational-gravitational fields are interchangeable. Consequently, the gravitational force density mirrors a comparable structure to that of the electric force density and the magnetic force density. The three spatial components of the Force-Density vector arising from the Electro-Magnetic-Gravitational interaction can be expressed as:

Intrinsic Equilibrium Electromagnetic-Gravitational Field Equation

$$\overline{f_{AA}} = -\frac{1}{c^2}\frac{\partial\,(\overline{E_A}\times\overline{H_A})}{\partial t} + \varepsilon_0\,\overline{E_A}\,(\nabla\cdot\overline{E_A}) - \varepsilon_0\,\overline{E_A}\times(\nabla\times\overline{E_A}) +$$

$$+\mu_0\,\overline{H_A}\,(\nabla\cdot\overline{H_A}) - \mu_0\,\overline{H_A}\times(\nabla\times\overline{H_A}) + \gamma_0\,\overline{g_A}\,(\nabla\cdot\overline{g_A}) - \gamma_0\,\overline{g_A}\times(\nabla\times\overline{g_A}) = 0\ [N/m^3] \qquad 6.1$$

Electromagnetic-Gravitational Coupling Field Equation (6)

$$\overline{f_{AB}} = -\frac{1}{c^2}\frac{\partial\,(\overline{E_A}\times\overline{H_A})}{\partial t} - \frac{1}{c^2}\frac{\partial\,(\overline{E_B}\times\overline{H_B})}{\partial t} + \varepsilon_0\,\overline{E_A}\,(\nabla\cdot\overline{E_B}) - \varepsilon_0\,\overline{E_A}\times(\nabla\times\overline{E_B}) +$$

$$+\mu_0\,\overline{H_A}\,(\nabla\cdot\overline{H_B}) - \mu_0\,\overline{H_A}\times(\nabla\times\overline{H_B}) + \gamma_0\,\overline{g_A}\,(\nabla\cdot\overline{g_B}) - \gamma_0\,\overline{g_A}\times(\nabla\times\overline{g_B})\ [N/m^3] \qquad 6.2$$

in which:

$\varepsilon_0\,(\nabla\cdot\overline{E}) = \rho_E$ Electric Charge Density $[C/m^3]$

$\mu_0\,(\nabla\cdot\overline{H}) = \rho_M$ Magnetic Flux Density $[Vs/m^3]$ or $[Wb/m^3]$

$\gamma_0\,(\nabla\cdot\overline{g}) = \rho_M$ Mass Density (Electromagnetic) $[kg/m^3]$

Electric Energy Density: $w_E = \frac{1}{2}\varepsilon_0 E^2$

Magnetic Energy Density: $w_M = \frac{1}{2}\mu_0 H^2$

Gravitational Energy Density: $w_G = \frac{1}{2}\gamma_0 g^2$

Equation (6) represent the two mutual "Gravitational-Electromagnetic Force Density Interactions" related to mass densities and energy densities. Kerr, R.P., Schild, A (2009) [31].

In which E represents the electric field intensity expressed in [V/m], H represents the magnetic field intensity expressed in [A/m] and g represents the gravitational acceleration expressed in $[m/s^2]$. The permittivity indicated as, ε_0 the permeability indicated as μ_0 and the gravitational permeability of vacuum as γ_0 .
Gobbi Julio (2018) [30] , Vegt W. (2002) [9] and Vegt W. (26-Oct-2022) [10].

The initial term in equation (6) portrays the inertia inherent in electromagnetic radiation. Additionally, the time derivative of the Poynting vector is included to represent the inertia term associated with the momentum of electromagnetic radiation. Vegt W. (26-Oct-2022) Equation: (25, 26) [12]

The succeeding terms, two and three, denote the interaction between electric fields. Subsequently, the fourth and fifth terms represent the interaction of magnetic fields and the sixth and seventh terms pertain to gravitational field interactions.

At the heart of this newly suggested theory resides a fundamental notion of universal equilibrium Joel Kaye (April 2014) [35] , demonstrating a pervasive presence across temporal, directional, and spatial dimensions. This overarching equilibrium finds concise representation through the zero-vector placed on the right-hand side of the equality symbol. One example of illustrating three-dimensional universal equilibrium is similar to the projection of a slide onto a screen (Vegt W. 2023) [4].

In the realm of curl-free gravitational fields Weng Zihua (2008) [25] and Mavromatos N. (2023) [29] , equation (6) is identical to equation (22) delineated in References(John G. Williamson, 2019) [11] and [25]. In the context of curl-free gravitational fields Weng Zihua, (October 2008) [25] and Mavromatos N. (2023) [29], equation (6) may be reformulated as follows:

$$\bar{f} = -\frac{1}{c^2}\frac{\partial(\bar{E}\times\bar{H})}{\partial t} + \varepsilon_0\,\bar{E}\,(\nabla\cdot\bar{E}) - \varepsilon_0\,\bar{E}\times(\nabla\times\bar{E}) + \tag{7}$$

$$+\mu_0\,\bar{H}\,(\nabla\cdot\bar{H}) - \mu_0\,\bar{H}\times(\nabla\times\bar{H}) + \bar{g}\,\rho_M = \bar{0}\quad [N/m^3]$$

Substituting Einstein's $W = m\,c^2$ in (7) results in "Electro-Magnetic-Gravitational Equilibrium Field Equation" (8) Vegt W. (2 Oct, 2021) [10] , Vegt W. (14 October 2022) [11] and Vegt Wim (26-Oct-2022) [12]:

$$\bar{f} = -\frac{1}{c^2}\frac{\partial(\bar{E}\times\bar{H})}{\partial t} + \varepsilon_0\,\bar{E}\,(\nabla\cdot\bar{E}) - \varepsilon_0\,\bar{E}\times(\nabla\times\bar{E}) + \tag{8}$$

$$+\mu_0\,\bar{H}\,(\nabla\cdot\bar{H}) - \mu_0\,\bar{H}\times(\nabla\times\bar{H}) + \frac{1}{2\,c^2}\bar{g}\left(\varepsilon E^2 + \mu H^2\right) = \bar{0}\quad [N/m^3]$$

The theory describes "Electromagnetic-Gravitational Interaction", "Magnetic-Gravitational Interaction" and "Electric-Gravitational Interaction". In this new theory particles do not interact with fields. The interaction between an electric charged particle and an electric field is not the interaction between a particle and a field but it is the interaction between the electric field of the particle interacting with the other electric field. Every interaction is an interaction between fields. Electric Fields interact with Electric Fields , Magnetic Fields interact with Magnetic Fields and Gravitational Fields only interact with Gravitational Fields and Vegt, Wim (1995) [3]

The consequence thereof is the dissemination of light (Electromagnetic Radiation) at the precise velocity of light ascertained by an Electro-Magnetic Perfect Equilibrium in all directions, at any given point, and at any temporal juncture.
Vegt Wim (Calculation 1, June 21, 2022) [15] posited this notion. This principle stands in opposition to Maxwell's theory of Electrodynamics, within which the speed of light is exclusively applicable to planar electromagnetic waves. Maxwell James Clerk (01 January 1865) [6]. The concept of the Universal Perfect Equilibrium transcends such limitations, applying to all manifestations of light, ranging from Laser Beams to the imagery depicting the genesis of the Universe.

3. Validation of the LIFE Framework in Accelerated Frames: From Macroscopic Gradients to Tokamak Dynamics

A fundamental requirement for any unified field equation applied to Tokamak confinement is its rigorous validity in highly accelerated, non-inertial coordinate systems. In magnetic fusion plasmas, both the physical fluid mass and the injected electromagnetic waves (such as the microwave frequencies used in Electron Cyclotron Resonance Heating, ECRH) are subjected to extreme, continuous accelerations. Because the LIFE framework establishes a strict dimensional equivalence between gravitational acceleration and electromagnetically induced kinematic acceleration (both functioning as N/m^3 force densities), macroscopic gravitational wave-propagation experiments serve as direct empirical validations for the theory's localized plasma dynamics.

To validate the underlying wave-propagation mechanics of the LIFE theory in an accelerated reference frame, the high-precision Gravitational-Redshift experiment conducted by (Herrmann S. Finke F. Lülf M. Kichakova O. et. Al. 2018) [2] was analysed. While performed using Galileo satellites, the core physics of this experiment represents the propagation of a highly stable microwave frequency (a MASER) through a varying continuous acceleration gradient. In the context of nuclear fusion, this mechanism is mathematically isomorphic to a gyrotron-emitted microwave beam traversing the intense radial electromagnetic and pressure gradients of a Tokamak to heat the dense plasma core.

By evaluating the frequency shift of the emitted wave, the experiment successfully compensates for orbital eccentricity and isolates the effect of the acceleration field. To apply this to the LIFE framework, we assume a generalized macroscopic acceleration field **g[z]**—representing either the gravitational gradient in the satellite experiment or the equivalent radial acceleration gradient within a fusion confinement vessel—dependent strictly on the radial direction **z** in Cartesian coordinates:

Assuming a gravitational field g[z] depending on the radial direction in cartesian coordinates between the ground station and the satellites:

$$\overline{g[z]} = \left\{0,0, \frac{G\, M_{Earth}}{4\, \pi\, z^2}\right\} \tag{9}$$

In which G ($G = 6.67428\ 10^{-11}\ Nm^2 / kg^2$) equals the Gravitational constant, M_{Earth} the mass of the earth and r the radial distance from the centre of the earth. The mathematical solution (Vegt W. 2023) [5] of equation (8) for plane electromagnetic waves (expressed in cartesian {x,y,z} coordinates) related to the Electric Field Intensity equals:

$$\overline{E} = \begin{pmatrix} E_x \\ E_y \\ E_z \end{pmatrix} = \begin{pmatrix} e^{-\frac{G\, M_{Eearth}\ \varepsilon_0\ \mu_0}{8\, \pi\, z}}\ h\left[\ \omega_0\ e^{-\frac{G\, M_{Earth}\ \varepsilon_0\ \mu_0}{4\, \pi\, z}}\left(t - \sqrt{\varepsilon\ \mu}\ z\right)\ \right] \\ 0 \\ 0 \end{pmatrix} \tag{10}$$

And the mathematical solution of (8) for the Magnetic Field Intensity equals:

$$\overline{H} = \begin{pmatrix} H_x \\ H_y \\ H_z \end{pmatrix} = \begin{pmatrix} 0 \\ \frac{1}{\sqrt{\varepsilon_0\ \mu_0}}\ e^{-\frac{G\, M_{Earth}\ \varepsilon_0\ \mu_0}{8\, \pi\, z}}\ h\left[\ \omega_0\ e^{-\frac{G\, M_{Earth}\ \varepsilon_0\ \mu_0}{4\, \pi\, z}}\left(t - \sqrt{\varepsilon\ \mu}\ z\right)\ \right] \\ 0 \end{pmatrix} \tag{11}$$

In which ω_0 equals the original frequency of the MASER radiation propagating in the direction of the gravitational field g[z] of the Earth in the z-direction. The exponential term demonstrates the Gravitational Redshift when the MASER radiation propagates in the direction of the Gravitational Field of the earth. The propagation speed of the Electromagnetic Radiation remains constant (the speed of light). But the amplitude of the field intensity and the frequency of the field intensity diminishes exponentially.

Calculations in Mathematica (Vegt W. 2023) [5] demonstrate a difference between the calculation with General Relativity and the calculation with the New Theory. Choosing for the ground station a distance to the centre of the earth $Z_1 = 6{,}378{,}000$ [m] (Radius of the Earth) and for the average distance of the ESA satellites in a Galileo orbit $Z_2 = 23{,}222{,}000$ [m] (distance from the ESA satellite to

the centre of the Earth), calculated with Mathematica, the Gravitational RedShift according General Relativity equals:

$$\Delta\,\omega_{GR} = 0.000000000040118\,15497097883\ [s^{-1}] \qquad (12)$$

Calculated with Mathematica, the Gravitational RedShift according the New Theory, which is a solution of equation (8) equals:

$$\Delta\,\omega_{GR} = 0.000000000040118\,24206173742\ [s^{-1}] \qquad (13)$$

Both calculated values a within the Range of the measured gravitational RedShift by the average values of both ESA satellites in the Galileo orbit

$$\Delta\,\omega_{Measured} = 0.000000000040118 \pm 2.2\ 10^{-15}\ [s^{-1}] \qquad (14)$$

In (Herrmann S. Finke F. Lülf M. Kichakova O. et. Al. 2018) [2] a factor α has been defined which presents the measured deviation α between the predicted Gravitational RedShift by General Relativity and the Measured Gravitational RedShift.

$$\alpha = \Delta\,\omega_{MEASURED} - \Delta\,\omega_{GR} = (2.2 \pm 1.6) \times 10^{-5} \qquad (15)$$

A comparable factor α can be used to determine which theory (General Relativity or the New Theory) has the nearest approach to the experimentally measured data. Highly accurate measuring experiments are required with an accuracy higher than 16 digits beyond the decimal point.

3 Energy Confinements by resonance in 3-D Eigenmodes based on LIFE theoretical Framework

A second fundamental solution for equation (8) describes a Gravitational Electromagnetic Confinement (BLACK HOLE) (Wheeler J. A. 1955) [1] within a radial gravitational field with acceleration g (in radial direction). This solution represents a Black Hole, the confinement of light due to its own gravitational field, and has no singularities. This solution for equation (8) describes Black Holes, dependent of time and radius, presenting discrete spherical energy levels, within a radial gravitational field with acceleration g (in radial direction) (Vegt W. 2022) [12] has been represented in (16) and (17).

$$\begin{pmatrix} E_r \\ E_\theta \\ E_\varphi \end{pmatrix} = \begin{pmatrix} 0 \\ f(r)\,\mathrm{Sin}(k\,r)\,\mathrm{Sin}(\omega\,t) \\ -f(r)\,\mathrm{Cos}(k\,r)\,\mathrm{Cos}(\omega\,t) \end{pmatrix} \quad \begin{pmatrix} H_r \\ H_\theta \\ H_\varphi \end{pmatrix} = \sqrt{\frac{\varepsilon}{\mu}} \begin{pmatrix} 0 \\ -f(r)\,\mathrm{Sin}(k\,r)\,\mathrm{Cos}(\omega\,t) \\ -f(r)\,\mathrm{Cos}(k\,r)\,\mathrm{Sin}(\omega\,t) \end{pmatrix} \quad \bar{g} = \begin{pmatrix} \frac{G_1}{4\,\pi\,r^2} \\ 0 \\ 0 \end{pmatrix} \qquad (16)$$

$$w_{em} = \left(\frac{\mu_0}{2} \left(\bar{m} \,.\, \bar{m} \right) + \frac{\varepsilon_0}{2} \left(\bar{e} \,.\, \bar{e} \right) \right) =$$

$$f(r)^2 \left(\left(\mathrm{Sin}(k\,r)\,\mathrm{Sin}(\omega\,t) \right)^2 + \left(\mathrm{Cos}(k\,r)\,\mathrm{Cos}(\omega\,t) \right)^2 + \frac{\varepsilon}{\mu} \left(\mathrm{Sin}(k\,r)\,\mathrm{Cos}(\omega\,t) \right)^2 + \left(\mathrm{Cos}(k\,r)\,\mathrm{Sin}(\omega\,t) \right)^2 \right)$$

In which the radial function f(r) equals:

$$f[r] = K\, e^{-\frac{G\, M_{BH}\, \varepsilon_0\, \mu_0}{8\,\pi\,r}} \qquad (17)$$

G represents the Gravitational constant and M represents the total confined electromagnetic mass of the BLACK HOLE. Equation (16) presents a Standing (Confined) Electromagnetic Field Configuration with a phase shift of 90 degrees between the electric field and the magnetic field with the corresponding Nodes and AntiNodes. (Vegt W. 2022) [11]. The solution has been calculated according Newton's Shell Theorem, resulting in the fundamental concept of the "Prima Materia" [43]

Assuming a constant speed of light "c" and Planck's constant ħ within the BLACK HOLE, the radius "R" (with n = 1,2,3,4….) of the BLACK HOLE with the energy of a proton, according $W = m_{proton}\, c^2$, would be: $1.5009211 \times 10^{-10}$ [J].

$$R_{GEON} = n\,\lambda = n\left(\frac{c}{f}\right) = n\left(\frac{c}{W}\right)\hbar = 7.1865\ 10^{-26}\left(\frac{n}{W}\right) \tag{18}$$

$$R_{GEON} = n\ 3.82\ 10^{-12}\ [m]$$

Black Holes are varying from atomic dimensions with dimensions of 10^{-27} [kg], Page 39 [33] until Black Holes with dimensions of 10^{40} [kg], Page 67 [34]. At these dimensions Black Holes turn into Dark Matter. The fundamental boundary condition for the confinement of Electromagnetic radiation (BLACK HOLEs) is that the energy flow (Poynting vector) $\bar{S} = \bar{E} \times \bar{H}$ equals zero at the surcface of the confinement. This is possible at every *"90 degrees Phase Shift Surface"* (*Sphere*) between the Electric Field and the Magnetic Field.

4 The relationship between Resonance in specific Eigenmodes and Quantum Mechanics

Introducing the Quantum Vector Function $\bar{\phi}$,

$$\bar{\phi} = \sqrt{\frac{\mu}{2}}\left(\bar{H} + i\,\frac{\bar{E}}{c}\right) \tag{19}$$

Substituting (21) in (16) results in the quantum presentation for the BLACK HOLE:

$$\overline{\Phi(r,\theta,\varphi)} = \sqrt{\frac{\mu}{2}}\left(\bar{H} + i\,\frac{\bar{E}}{c}\right) f(r)\begin{pmatrix}\Phi_r\\ \Phi_\theta\\ \Phi_\varphi\end{pmatrix} \tag{20}$$

$$\overline{\Phi(r,\theta,\varphi)} = K\sqrt{\frac{\varepsilon}{\mu}}\,e^{-\frac{G1\,\varepsilon_0\,\mu_0}{8\,\pi\,r}}\begin{pmatrix}0 & 0 & 0\\ 0 & -\mathrm{Sin}(k\,r) & \mathrm{Sin}(k\,r)\\ 0 & -i\,\mathrm{Cos}(k\,r) & i\,\mathrm{Cos}(k\,r)\end{pmatrix}\begin{Bmatrix}0\\ \mathrm{Cos}\,(\omega\,t)\\ i\,\mathrm{Sin}\,(\omega\,t)\end{Bmatrix}$$

With "K" a constant value dependend of the mass of the BLACK HOLE. The Dot product between the unit vector and the Quantum Vector Function $\bar{\phi}$ represents the quantum mechanical probability function $\Psi[r,t]$ which is a fundamental solution of the Schrödinger Wave Equation. (Vegt, J. W. 1995) [3]

$$\overline{\Phi(r,\theta,\varphi)} = K \sqrt{\frac{\varepsilon}{\mu}}\, e^{-\frac{G1\,\varepsilon_0\,\mu_0}{8\,\pi\,r}} \begin{pmatrix} 0 & 0 & 0 \\ 0 & -\mathrm{Sin}(k\,r) & \mathrm{Sin}(k\,r) \\ 0 & -i\,\mathrm{Cos}(k\,r) & i\,\mathrm{Cos}(k\,r) \end{pmatrix} \begin{Bmatrix} 0 \\ \mathrm{Cos}\,(\omega\,t) \\ i\,\mathrm{Sin}\,(\omega\,t) \end{Bmatrix} \tag{21}$$

$$\Psi(r,t) = \begin{Bmatrix} 1 & 1 & 1 \end{Bmatrix} \begin{Bmatrix} 0 \\ \mathrm{Cos}\,(\omega\,t) \\ i\,\mathrm{Sin}\,(\omega\,t) \end{Bmatrix} K \sqrt{\frac{\varepsilon}{\mu}}\, e^{-\frac{G1\,\varepsilon_0\,\mu_0}{8\,\pi\,r}} = K \sqrt{\frac{\varepsilon}{\mu}}\, e^{-\frac{G1\,\varepsilon_0\,\mu_0}{8\,\pi\,r}}\, e^{i\,\omega\,t}$$

The Scalar function $\Psi[r,t]$ represents a fundamental solution of the Quantum Mechanical Schrödinger wave equation. [36, 37]

4.1 Eigenmodes with Discrete Spherical Energy Levels at Sub-Atomic dimensions

A crucial criterion for effectively confining Electromagnetic Energy entails ensuring that the Poynting vector equates to zero at the spherical surface delineating the confines. Specifically, to encapsulate this energy within a sphere, the setup necessitates a standing electromagnetic wave configuration characterized by concentric spheres. At each sphere boundary, there exists an antinodal plane for either the Electric Field (E) or Magnetic Field (B), with a radial distance separating each sphere that corresponds to half the wavelength of the taken confinement. The relationship is governed by the defined constant $k = n\pi\lambda$, where "n" pertains to a natural number sequence (1, 2, 3, 4, and so forth), and λ signifies the wavelength of the electromagnetic wave being considered.

4.1.1 Time and Radius dependent Eigenmodes with discrete Energy Levels. The confinements of Electromagnetic Radiation within spherical Regions.

Each concentric sphere serves as an antinodal surface for either the Electric Field (E) or the Magnetic Field (H). At these boundaries, the Poynting Vector^ is precisely zero at any given time and location within the sphere. Notably, the confinement ensures that Electromagnetic Energy remains contained within the boundaries of each sphere and transitions seamlessly to the subsequent concentric sphere. The distinctive property of these concentric spheres lies in the variance of their radii, set at one half wavelength of the electromagnetic radiation within the enclosure, reflecting discrete energy levels. It is important to note that each concentric sphere functions as an antinodal surface for either the electric or magnetic field, contributing to the structured confinement of electromagnetic energy within the system.

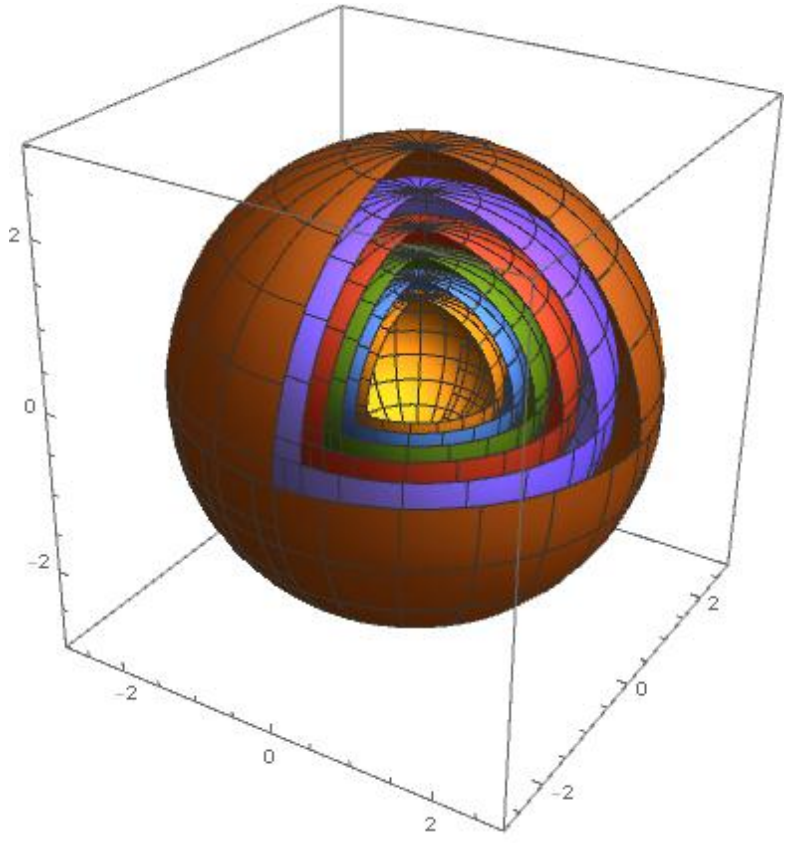

Fig. 5 Nodal and Antinodal Spheres for Standing (Confined) Spherical Electromagnetic waves with a 90 degrees phase shift between the Electric field and the Magnetic field. Equation (9)

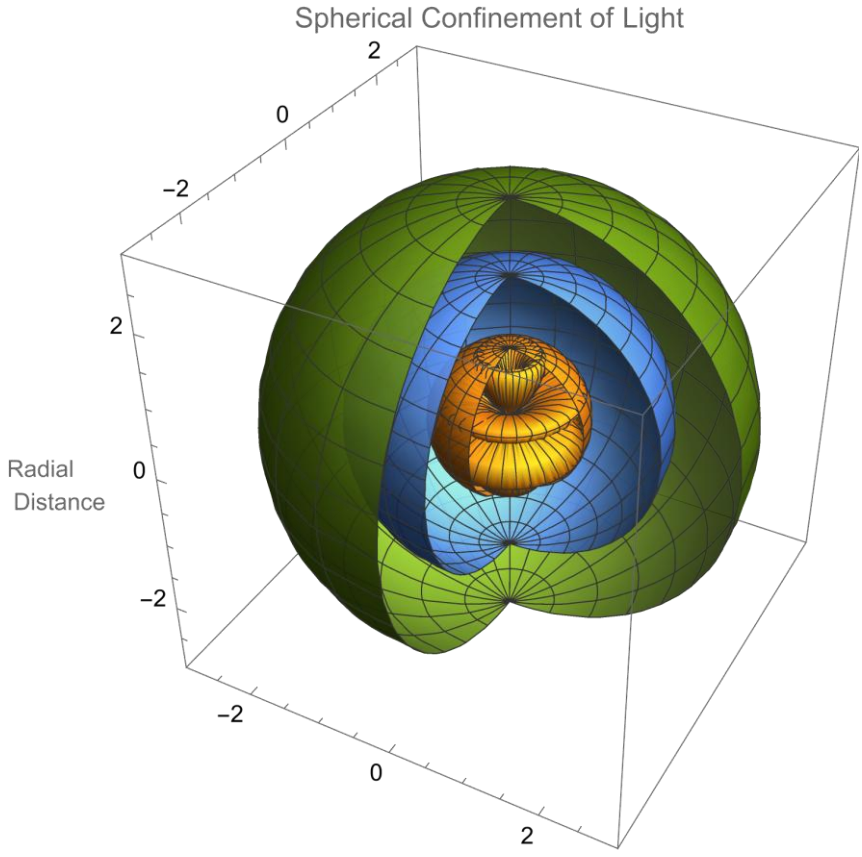

Fig. 6 Nodal- and Antinodal Spheres (k = 3) for Standing (Confined) Spherical Electromagnetic waves with a 90 degrees phase shift between the Electric field and the Magnetic field. Equation (9)

Equation (24) describes a Time and Radius dependent BLACK HOLE.

$$\overline{E} = K\, e^{-\frac{G1\varepsilon 0\mu 0}{8\pi r}} \begin{pmatrix} 0 \\ \text{Sin}[k\ r]\ \text{Sin}[\omega\ t] \\ -\text{Cos}[k\ r]\ \text{Cos}[\omega\ t] \end{pmatrix}$$

$$\overline{H} = K\, e^{-\frac{G1\epsilon 0\mu 0}{8\pi r}} \sqrt{\frac{\varepsilon_0}{\mu_0}} \begin{pmatrix} 0 \\ \text{Sin}[k\ r]\ \text{Cos}[\omega\ t] \\ -\text{Cos}[k\ r]\ \text{Sin}[\omega\ t] \end{pmatrix} \tag{22}$$

Equation (20) represents by the function $\mathrm{Sin}[k\,r]$ (k = 1,2,3,4….) the confinement of electromagnetic radiation between two concentric spheres. K represents the amplitude of the Electric/ Magnetic Field Intensty. (Vegt W. 2022) [13]

4.1.2 Time and Polar Angle dependent Eigenmodes

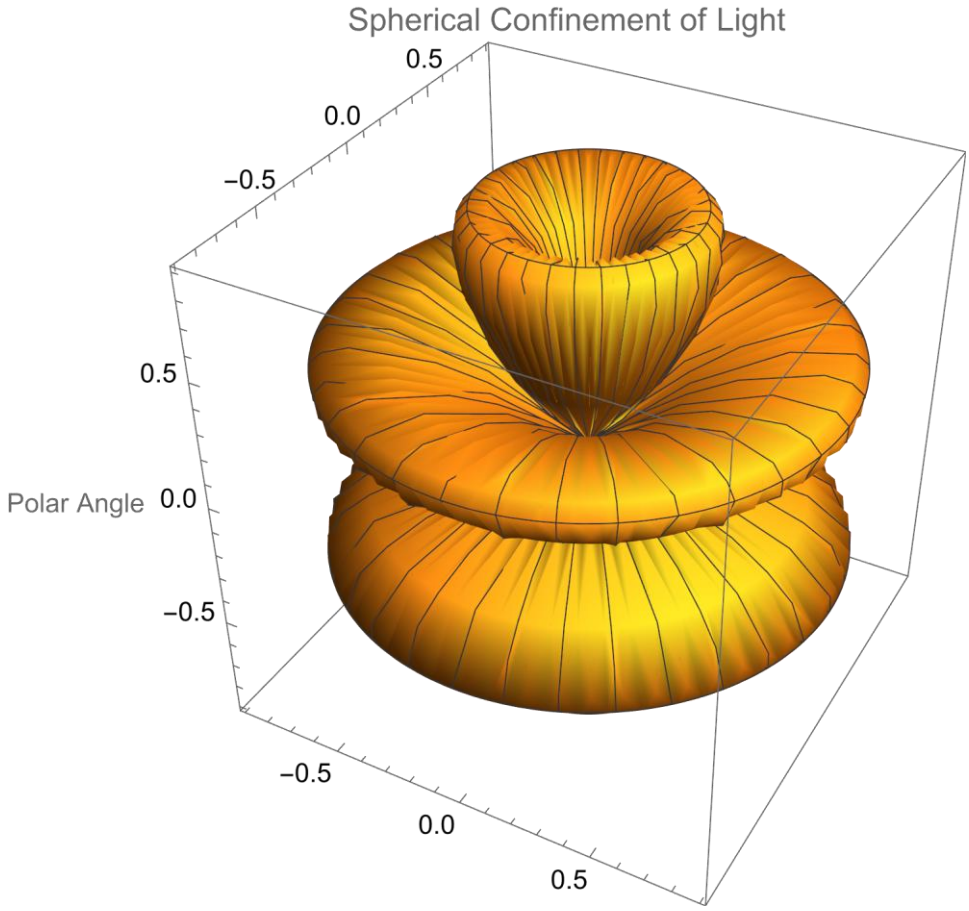

Fig. 7 Nodal- and Antinodal Polar Angle Regions (m = 3) for Standing (Confined) Spherical Electromagnetic waves with a 90 degrees phase shift between the Electric field and the Magnetic field. Equation (15)

Equation (25) describes a Time and “Polar Angle” dependent BLACK HOLE

$$\overline{E} = K\, e^{-\frac{G1\varepsilon 0\mu 0}{8\pi r}} \begin{pmatrix} 0 \\ \text{Sin}[m\ \theta]\ \text{Sin}[\omega\ t] \\ \text{Sin}[m\ \theta]\ \text{Cos}[\omega\ t] \end{pmatrix} \tag{23}$$

$$\overline{H} = K\, e^{-\frac{G1\epsilon 0\mu 0}{8\pi r}} \sqrt{\frac{\varepsilon_0}{\mu_0}} \begin{pmatrix} 0 \\ \text{Sin}[m\ \theta]\ \text{Cos}[\omega\ t] \\ -\text{Sin}[m\ \theta]\ \text{Sin}[\omega\ t] \end{pmatrix}$$

Equation (19) represents by the function $\text{Sin}[m\,\theta]$ (m = 1,2,3,4…..) the confinement of electromagnetic radiation between two Polar Angular Regions [15].

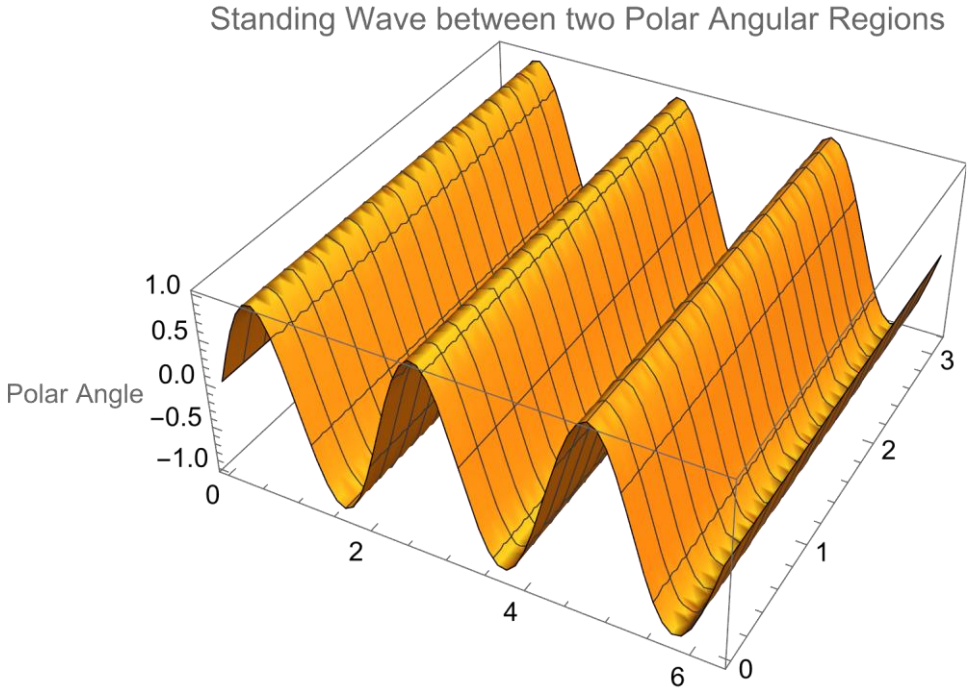

Fig. 8 Nodal- and Antinodal Polar Angle Regions (m = 3) for Standing (Confined) Electromagnetic waves with a 90 degrees phase shift between the Electric field and the Magnetic field. Equation (15)

4.1.3 Time and Azimuthal Angular dependent Eigenmodes

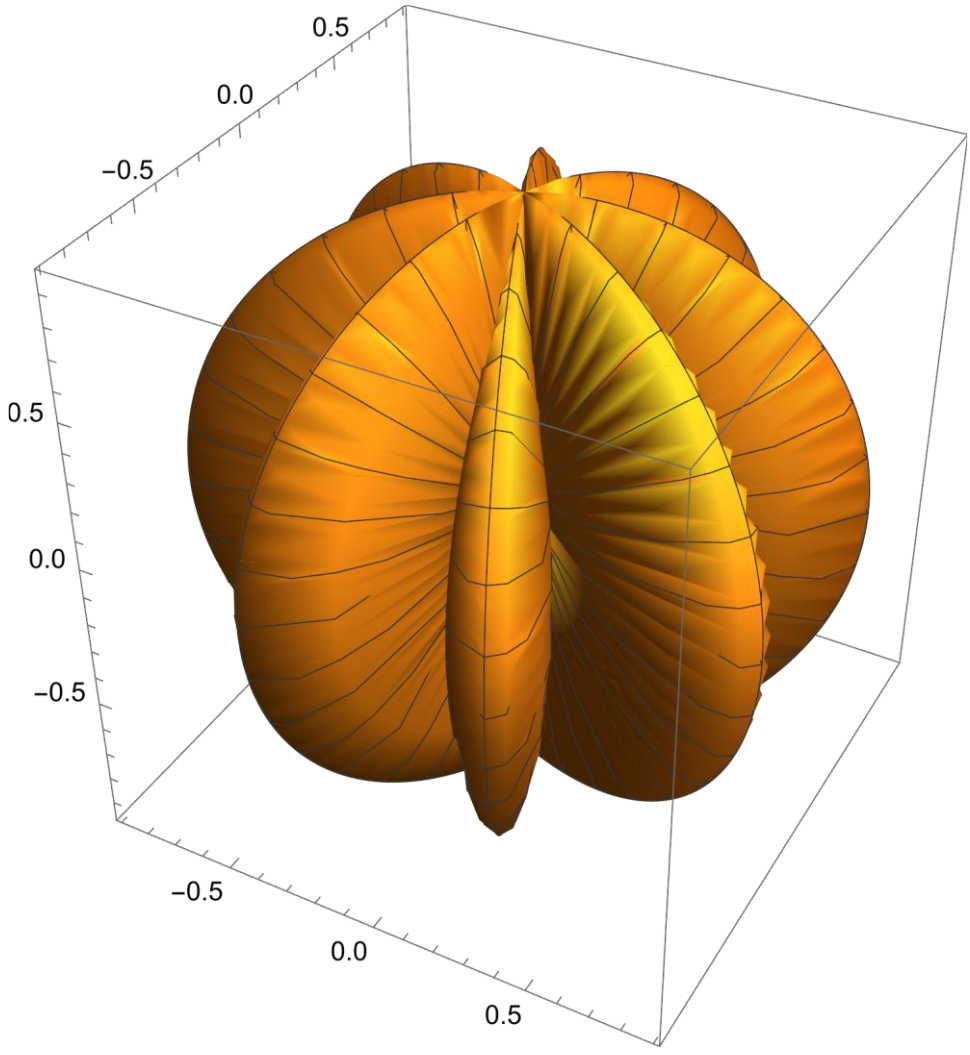

Fig. 9 Nodal- and Antinodal Azimuthal Angular Regions (n = 3) for Standing (Confined) Electromagnetic waves with a 90 degrees phase shift between the Electric field and the Magnetic field. Equation (16)

Equation (26) describes a Time and “Polar Angle” dependent BLACK HOLE

$$\overline{E} = K\, e^{-\frac{G1\varepsilon 0\mu 0}{8\pi r}} \begin{pmatrix} 0 \\ \text{Cos}[n\ \varphi]\ \text{Sin}[\omega\ t] \\ \text{Cos}[n\ \varphi]\ \text{Cos}[\omega\ t] \end{pmatrix} \tag{24}$$

$$\overline{H} = K\, e^{-\frac{G1\epsilon 0\mu 0}{8\pi r}} \sqrt{\frac{\varepsilon_0}{\mu_0}} \begin{pmatrix} 0 \\ \text{Cos}[n\ \varphi]\ \text{Cos}[\omega\ t] \\ -\text{Cos}[n\ \varphi]\ \text{Sin}[\omega\ t] \end{pmatrix}$$

Equation (26) represents by the function $\text{Sin}[n\ \varphi]$ (n = 1,2,3,4…..) the confinement of electromagnetic radiation between two Azimuthal Angular Regions (Vegt W. 2022) [15].

4.1.4 Time, Polar- and Azimuthal Angular dependent Eigenmmodes

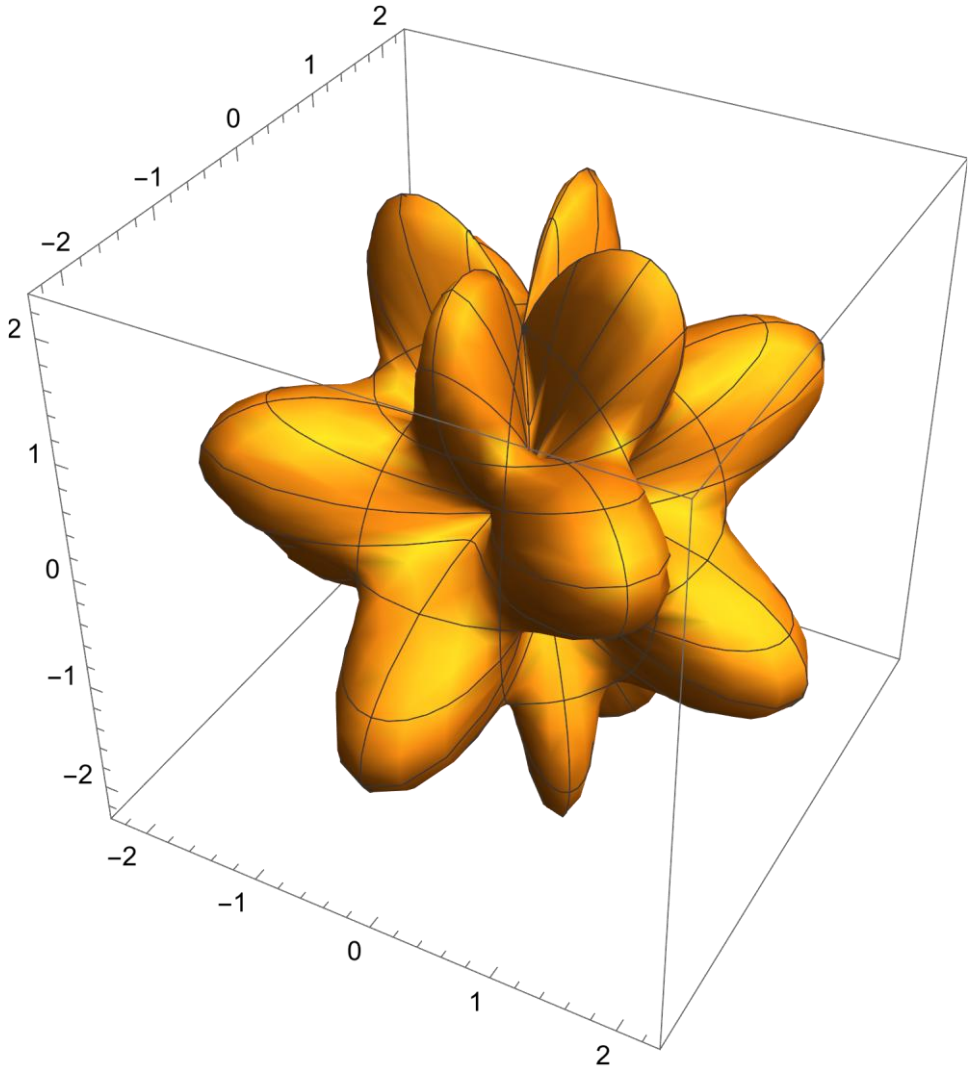

Fig. 10 Nodal- and Antinodal Polar Angular and Azimuthal Angular Regions (n = 4 and m = 4) for Standing (Confined) Electromagnetic waves with a 90 degrees phase shift between the Electric field and the Magnetic field. Equation (17)

Equation (27) describes a Time “Azimuthal Angle” and “Polar Angle” dependent Eigenmode for local energy confinement based on the LIFE theoretical framework.

$$\overline{E} = K\, e^{-\frac{G1\varepsilon 0\mu 0}{8\pi r}} \begin{pmatrix} 0 \\ \text{Cos}[n\ \varphi]\ \text{Sin}[m\ \theta]\ \text{Sin}[\omega\ t] \\ \text{Cos}[n\ \varphi]\ \text{Sin}[m\ \theta]\ \text{Cos}[\omega\ t] \end{pmatrix}$$

$$\overline{H} = K\, e^{-\frac{G1\epsilon 0\mu 0}{8\pi r}} \sqrt{\frac{\varepsilon_0}{\mu_0}} \begin{pmatrix} 0 \\ -\text{Cos}[n\ \varphi]\ \text{Sin}[m\ \theta]\ \text{Cos}[\omega\ t] \\ \text{Cos}[n\ \varphi]\ \text{Sin}[m\ \theta]\ \text{Sin}[\omega\ t] \end{pmatrix} \tag{25}$$

Equation (27) represents by the function $\text{Cos}[n\ \varphi]$ (n = 1,2,3,4…..) and $\text{Sin}[m\ \theta]$ (m = 1,2,3,4…..) the confinement of electromagnetic radiation between two Azimuthal Angular Regions and two Polar Angulars Regions . (Vegt W. 2022) [14]

4.1.5 Spherical Confinement of Electromagnetic Radiation beween two Concentric Spheres within gravitational confinements of radiation

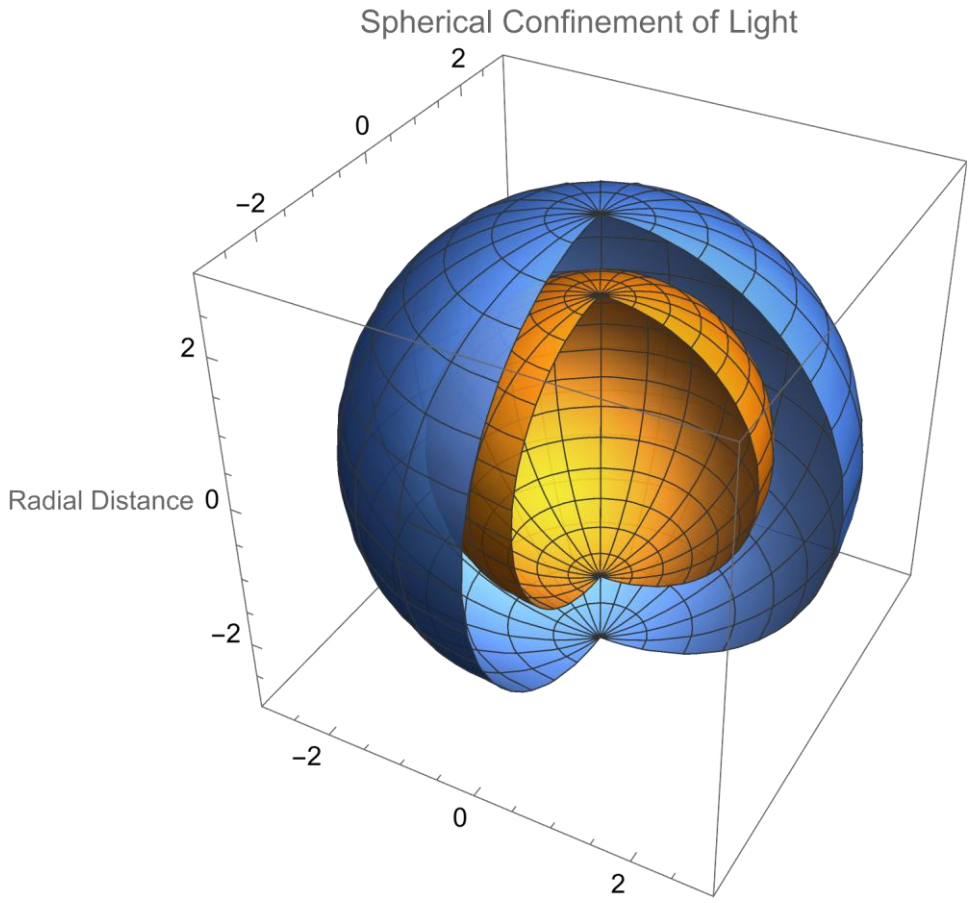

Fig.11 Nodal- and Antinodal Regions for Standing (Confined) Electromagnetic waves with a 90 degrees phase shift between the Electric field and the Magnetic field. Equation (14)

Equation (18) elucidates the mirrored propagation of the Confined Electromagnetic Energy within the BLACK HOLE, encompassed between two successive concentric spheres. Notably, the speed of light, contingent upon the variable "r," experiences alterations in direction concurrent with variations in the frequency of the confined light, representing the Electromagnetic Radiation. (Vegt W. 2022) [13]

In a transformative manner, a BLACK HOLE has the capacity to bifurcate into two distinctive entities, each characterized by a different radius. This metamorphosis manifests as the original BLACK HOLE regresses into a lower energy state, akin to an atom transitioning to a lower energy level. Concurrently, the emergence of the

new BLACK HOLE symbolizes the contrast in energy levels, mirroring the dynamics of an atom cascading to a lower energy state within its structure.

$$\bar{E} = K\, e^{-\frac{G1\varepsilon 0\mu 0}{8\pi r}} f\left[t - \frac{\sqrt{\varepsilon_0\ \mu_0}\ \text{Cos}[2\,k\,r]}{2\,k}\right] \begin{pmatrix} 0 \\ \text{Sin}[k\,r]\ \text{Sin}[\omega\,t] \\ -\text{Cos}[k\,r]\ \text{Cos}[\omega\,t] \end{pmatrix} \tag{26}$$

$$\bar{H} = K\, e^{-\frac{G1c0\mu 0}{8\pi r}} f\left[t - \frac{\sqrt{\varepsilon_0\ \mu_0}\ \text{Cos}[2\,k\,r]}{2\,k}\right] \sqrt{\frac{\varepsilon_0}{\mu_0}} \begin{pmatrix} 0 \\ -\text{Sin}[k\,r]\ \text{Cos}[\omega\,t] \\ -\text{Cos}[k\,r]\ \ \text{Sin}[\omega\,t] \end{pmatrix}$$

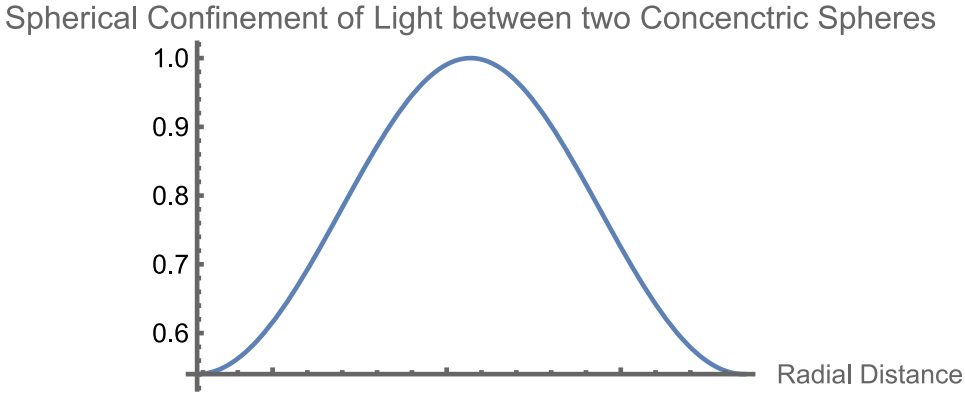

Fig. 12 Nodal- and Antinodal Regions for Standing (Confined) Electromagnetic within two concentric spheres. Equation (18)

5. Electro-Dynamic Directional Shift and Azimuthal Resonance of Injected MASER Beams

A critical requirement for establishing a three-dimensional macroscopic resonant cavity within a Tokamak is the continuous propagation of electromagnetic energy along the azimuthal (toroidal) axis. However, heating mechanisms such as Electron Cyclotron Resonance Heating (ECRH) typically rely on a MASER beam injected perpendicular (radially) to the macroscopic plasma flow. Within the Local Interaction Field Equilibrium (LIFE) framework, the phenomenon of a radially injected MASER beam changing direction to propagate alongside the azimuthal plasma flow is driven by the unified continuous coupling of electro-dynamic and fluid-dynamic force densities.

This directional shift and subsequent resonance occur through four integrated physical mechanisms:

5.1 The Fizeau Drag Effect in a Moving Plasma Dielectric

In classical optics, electromagnetic waves traveling through a moving medium experience a phase and group velocity "drag" in the direction of the medium's flow, known as the Fizeau effect. In a Tokamak, the ultra-dense fusion plasma acts as a highly refractive, turbulent dielectric fluid. Because the charged plasma particles move with immense kinetic velocity in the azimuthal direction, this moving refractive index inherently drags the perpendicularly injected MASER wave. As the microwave photons traverse the dense core, their propagation vector (**k**) gradually tilts from purely radial to partially azimuthal.

5.2 Direct Coupling of Volumetric Force Densities

Standard magnetohydrodynamic approaches treat the radiation pressure of the injected wave and the mechanical momentum of the plasma as distinct systems. The LIFE framework resolves this by strictly expressing both as unified volumetric force densities (N/m^3). When the radial electromagnetic force density of the MASER intersects the massive azimuthal mechanical force density of the flowing Deuterium plasma, the continuous mathematical boundary allows direct momentum transfer. The azimuthal momentum of the fluid continuously exerts a force density upon the electromagnetic wave, naturally bending its trajectory to align with the macroscopic fluid flow.

5.3 Relativistic Scattering and Aberration

As the MASER beam penetrates the plasma, its microwave photons [8] are continuously absorbed and re-emitted (scattered) by electrons via cyclotron

resonance. Because these electrons are traveling at extreme velocities along the azimuthal axis, any photon they re-emit experiences relativistic aberration. The emission profile is "beamed" forward in the direction of the electron's travel vector. Consequently, a photon absorbed from a radial trajectory is statistically re-emitted with a new velocity vector pointing azimuthally.

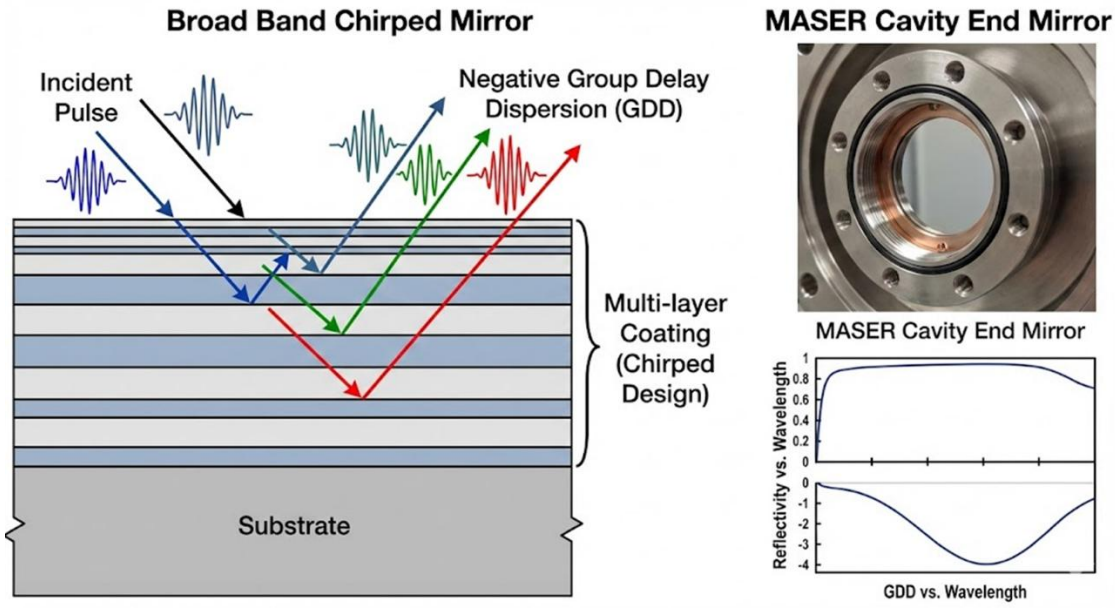

Figure 13: *Conceptual configuration of radial MASER injection into the Tokamak confinement vessel. A 100% reflective mirror is positioned on the inner wall opposite the injection port. This initial setup establishes the radial resonance required to concentrate maximum kinetic energy (velocity anti-node) at the plasma core, while maintaining minimum energy (velocity node) at the material boundaries.*

5.4 The Role of the Broadband Chirped Mirror in Azimuthal Amplification

To capture the directionally shifting wave and amplify it into a stable toroidal standing wave, a Broad Band Chirped Mirror featuring Negative Group Delay Dispersion (GDD) is implemented on the confinement wall opposite the MASER oscillator.

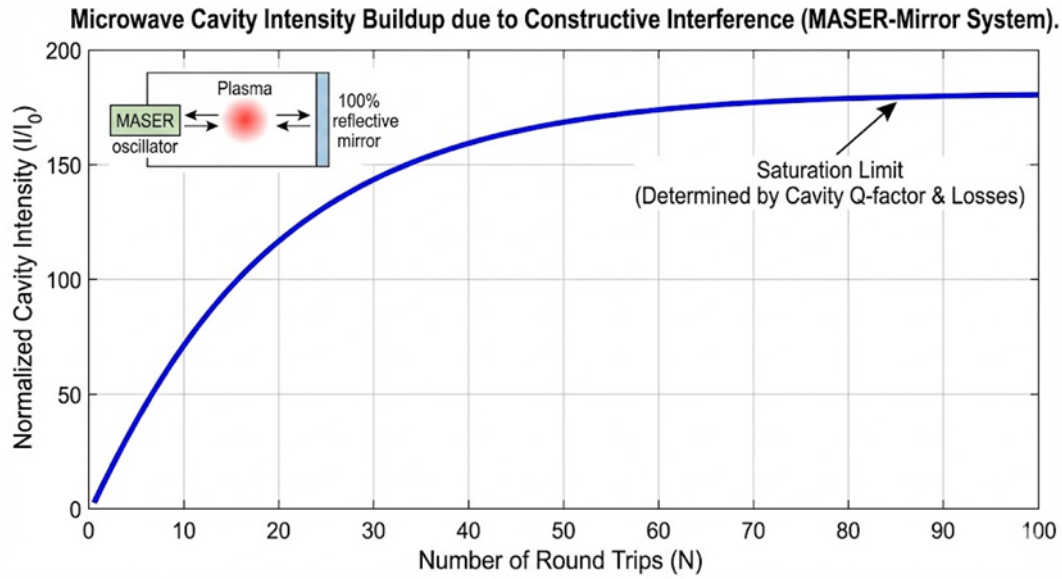

Figure 14: *Schematic representation of the Broad Band Chirped Mirror. The multi-layer dielectric coating is designed to provide Negative Group Delay Dispersion (GDD). As the microwave pulses are scattered and dispersed by the turbulent, high-velocity plasma, the chirped mirror compensates for this temporal broadening, restoring the integrity and phase coherence of the wave packet upon reflection.*

As the injected radial beam is dragged azimuthally by the mechanisms described above, it strikes the opposite wall at an oblique angle rather than purely perpendicularly. Upon reflection by the chirped mirror, this angle is preserved and compounded. As the electromagnetic wave undergoes multiple reflections across the highly refractive plasma cavity, the continuous azimuthal drag "pushes" the wave further along the toroidal axis with every pass.

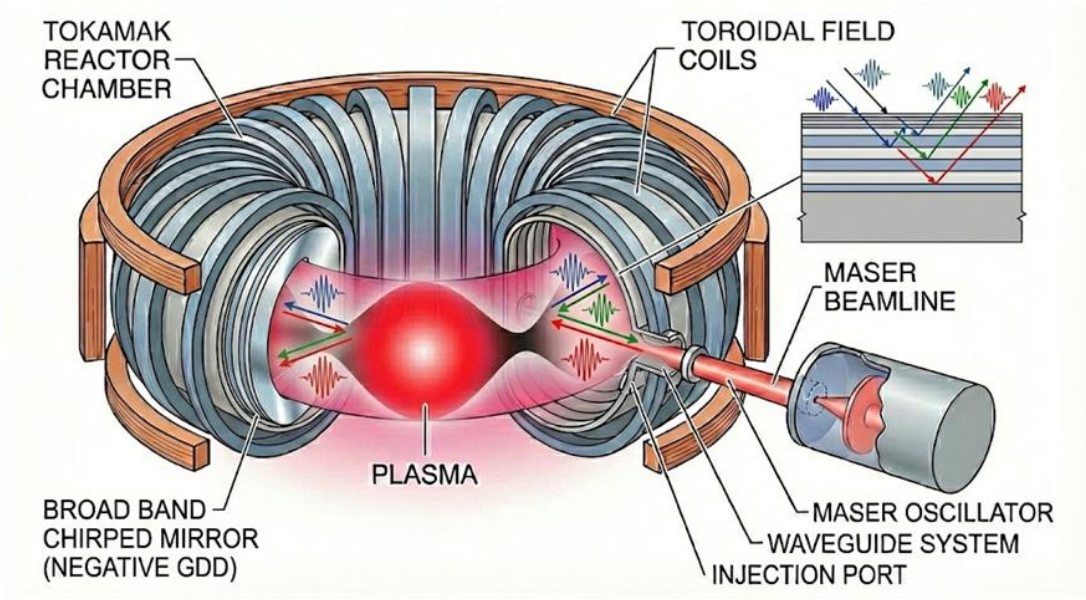

Figure 15: *Integrated LIFE confinement system demonstrating the continuous electro-dynamic directional shift. The radially injected MASER beam is continuously deflected by the azimuthal force density of the flowing plasma. The Broadband Chirped Mirror (Negative GDD), located opposite the injection port, reflects the deflected beam. Through successive reflections and continuous Fizeau drag, the electromagnetic energy successfully aligns with the azimuthal axis, fulfilling the boundary conditions required to establish a stable, three-dimensional toroidal standing wave.*

6 Universal Equilibrium in the "Concept of Quantum Mechanical Probability" in "LIFE".

The 4-dimensional notation for the divergence of the Stress-Energy Tensor (25) expresses in the 4th dimension (time dimension) the law of Conservation of Energy". For an Electromagnetic Field the law for conservation of Energy has been expressed as:

$$\bar{f}^4 = \begin{pmatrix} f_4 \\ f_3 \\ f_2 \\ f_1 \end{pmatrix} = \square \bullet \bar{\bar{T}} = \begin{pmatrix} \nabla \cdot \bar{S} + \frac{\partial w}{\partial t} \\ f_3 \\ f_2 \\ f_1 \end{pmatrix} = \bar{0}^4 \qquad (27)$$

From the derivation of the equation governing the "Conservation of Electromagnetic Energy" (38.1), we can extract the crux of the matter: the derivation of the "Fundamental Equation for Confined Electromagnetic Interaction" within "The New Theory." This fundamental equation aligns closely with the Relativistic Quantum Mechanical "Dirac" equation and the Schrödinger wave equation, particularly at velocities significantly lower in magnitude relative to the speed of light.

In essence, this "Fundamental Equation for Confined Electromagnetic Interaction" within "The Proposed Theory" essentially embodies a relativistic iteration of the Quantum Mechanical Schrödinger wave equation, effectively mirroring the attributes of the Quantum Mechanical Dirac Equation within the context of this modified theoretical framework.

7. Topological Resonance and 3-D Electromagnetic Field Configuration of the Toroidal Eigenmode

To mathematically satisfy the continuous boundary conditions required for the three-dimensional resonant cavity, the electromagnetic field intensities must form a stable, closed topological structure. By solving the intrinsic equilibrium equations for the electric ($\mathbf{e_v}$) and magnetic ($\mathbf{m_v}$) field vectors within the accelerated toroidal coordinate system, we derive a localized solitonic wave packet (John G. Williamson, 2019) [11]. The resulting 3-D field configuration (Figure 16) demonstrates the perfect geometrical resonance that prevents destructive interference and maintains the critical temperature gradients across the plasma profile.

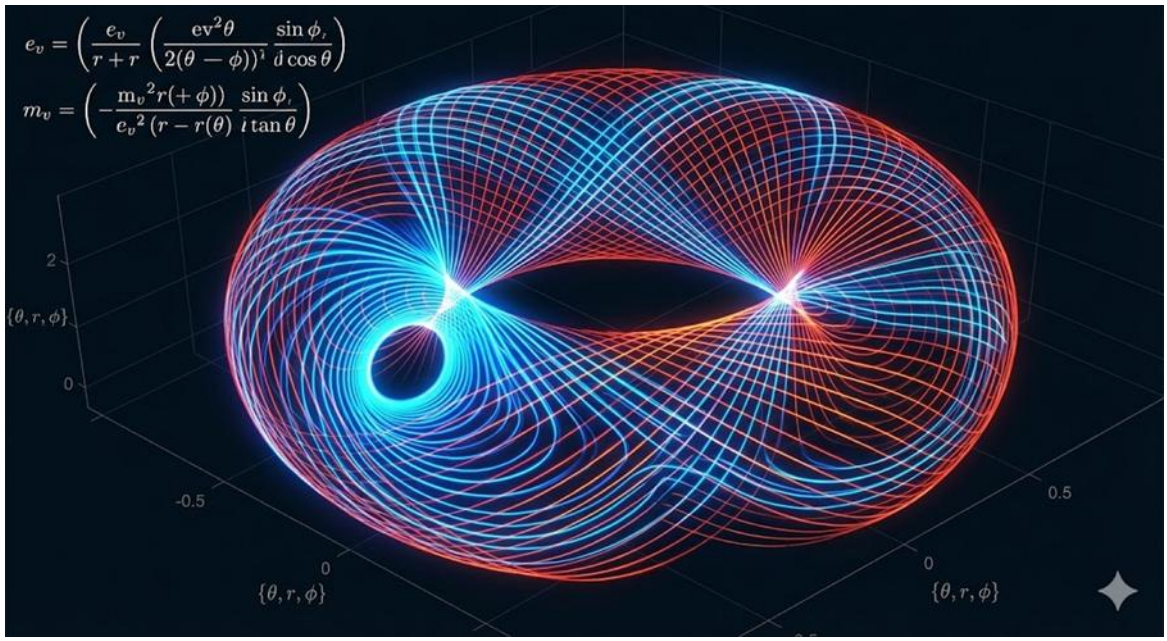

Figure 16: Three-dimensional topological visualization of the electromagnetic field configuration within the Local Interaction Field Equilibrium (LIFE) framework. The interlaced trajectories represent the exact spatial distribution of the electric field intensity ($\mathbf{e_v}$) and the corresponding magnetic field intensity ($\mathbf{m_v}$) required to form a macroscopic toroidal eigenmode. Governed by complex hyperbolic and trigonometric coordinate transformations, this mathematically closed-loop continuous field ensures absolute macroscopic boundary stability. The orthogonal but intrinsically coupled geometry of these fields generates the unified volumetric force densities (N/m^3) that drive the plasma confinement. This specific topological resonance is what fundamentally sustains the velocity anti-node (maximum kinetic temperature) at the magnetic axis while strictly enforcing the velocity node (minimum kinetic temperature) at the inner surface of the Tokamak vessel, thereby providing inherent thermal shielding.

7.1 Mathematical Formulation of the Electromagnetic Field Vectors

The exact three-dimensional topological field configuration depicted in Figure 16 is derived within a localized toroidal coordinate system (θ, r, ϕ), with the domain boundaries defined as:

$-\pi < \theta \leq \pi \quad (Poloidal\ angle)$

$0 \leq r < \infty \quad (Radial\ scale)$

$-\pi < \phi \leq \pi \quad (Azimuthal\ /\ Toroidal\ angle)$

To maintain macroscopic stability within the Local Interaction Field Equilibrium (LIFE) framework, the electric field intensity vector $\mathbf{e_v}$ and the magnetic field intensity vector $\mathbf{m_v}$ are rigorously defined as orthogonal, interlinked vector fields.

Intrinsic Equilibrium Electromagnetic LIFE Field Equation

$$\overline{f_{AA}} = -\frac{1}{c^2}\frac{\partial\,(\overline{E_A} \times \overline{H_A})}{\partial t} + \varepsilon_0\,\overline{E_A}\,(\nabla \cdot \overline{E_A}) - \varepsilon_0\,\overline{E_A} \times (\nabla \times \overline{E_A}) + \mu_0\,\overline{H_A}\,(\nabla \cdot \overline{H_A}) - \mu_0\,\overline{H_A} \times (\nabla \times \overline{H_A}) = 0 \ [N/m^3] \tag{28}$$

To improve the readability of the intrinsic equilibrium equations, we first define a foundational geometric phase function, $\Omega(r,\theta)$, which dictates the spatial curvature and boundary continuity of the localized wave packet:

$$\Omega(r,\theta) = r - 2\arctan\left(\coth\left(\frac{r}{2}\right)\tan\left(\frac{\theta}{2}\right)\right)\cot(\theta) + h(\theta)$$

(where $h(\theta)$ is an arbitrary continuous function of the poloidal angle).

This math allows us to create a 3-D macroscopic resonant cavity. Using this geometric phase function, along with integration constants $\mathbf{K_1}$ and $\mathbf{K_2}$, and the dynamic phase/amplitude modulation function $f_{13}(\theta, r, \phi, t)$, the exact components of the **Electric Field Intensity** (e_v) are defined as:

$$\mathrm{e}_v = \begin{pmatrix} \mathrm{e}_{v,\theta} \\ \mathrm{e}_{v,r} \\ \mathrm{e}_{v,\phi} \end{pmatrix} = \begin{pmatrix} 0 \\ \frac{1}{\sqrt{2}}(\cosh r - \cos\theta)^{3/2}\,\mathrm{csch}\, r\sqrt{K_1 - f_{13}^2}\sqrt{\Omega(r,\theta)} \\ (\cosh r - \cos\theta)\,\mathrm{csch}\, r \cdot f_{13}\sqrt{-K_2 + \frac{1}{2}(\cos\theta - \cosh r)\Omega(r,\theta) + \sinh r} \end{pmatrix} \tag{29}$$

Correspondingly, the exact components of the **Magnetic Field Intensity $\mathbf{m_v}$** are strictly coupled to the electric field via the admittance of free space $(\sqrt{\epsilon_0 / \mu_0})$ to ensure perfect dimensional and energetic equilibrium:

$$m_v = \begin{pmatrix} m_{v,\theta} \\ m_{v,r} \\ m_{v,\phi} \end{pmatrix} = -\sqrt{\frac{\epsilon_0}{\mu_0}} \begin{pmatrix} 0 \\ \frac{1}{\sqrt{2}}(\cosh r - \cos\theta)^{3/2}\,\mathrm{csch}\, r\sqrt{K_1 - f_{13}^2}\sqrt{\Omega(r,\theta)} \\ (\cosh r - \cos\theta)\,\mathrm{csch}\, r \cdot f_{13}\sqrt{-K_2 + \frac{1}{2}(\cos\theta - \cosh r)\Omega(r,\theta) + \sinh r} \end{pmatrix} \tag{30}$$

- (θ, r, ϕ): The toroidal coordinate system variables (poloidal angle, radial scale, and azimuthal angle).
- K_1, K_2: Constants of integration defining the steady-state boundary constraints.
- $f_{13} \equiv f_{13}(\theta, r, \phi, t)$: The dynamic phase and amplitude modulation function that governs the wave packet's spatiotemporal evolution.
- $(\cosh r - \cos\theta)$: The fundamental Lamé scale factor characteristic of toroidal geometry, ensuring that the field mathematically conforms to the Tokamak cavity.

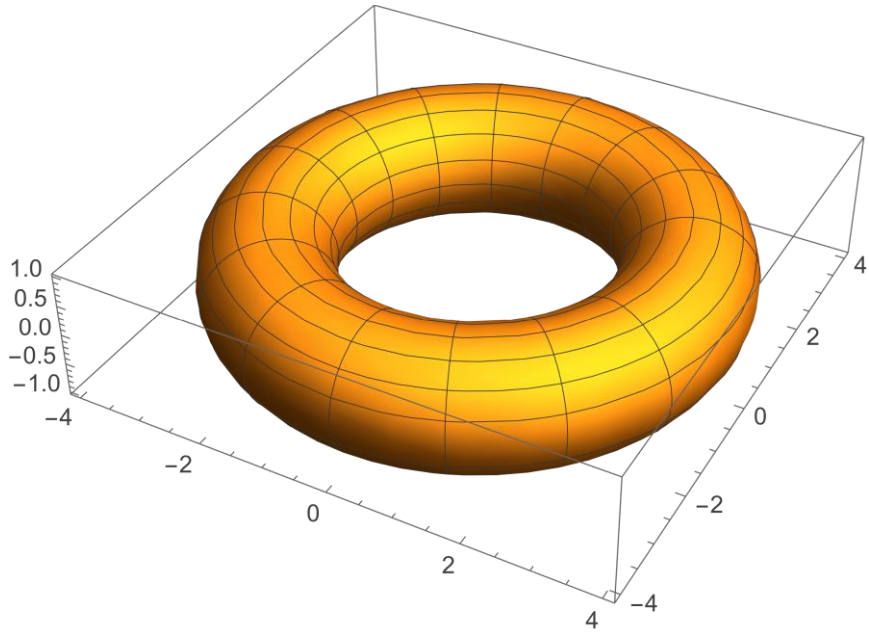

Figure 17: Computational visualization of the toroidal electromagnetic confinement generated via Wolfram Mathematica 11. The surface represents the continuous spatial envelope of the injected MASER radiation within the Tokamak cavity. Governed by the Local Interaction Field Equilibrium (LIFE) framework, the electric and magnetic field vectors orthogonally lock into a closed 3-D topological resonance. This mathematically proven zero-force-density configuration traps the microwave energy in a stable azimuthal loop, preventing radial dissipation and establishing the thermal gradients necessary for optimal fusion conditions.

7.2 Macroscopic Visualization of the Toroidal MASER Confinement

To geometrically visualize the zero-force-density equilibrium derived from the Local Interaction Field Equilibrium (LIFE) equations, the continuous spatial envelope of the electromagnetic field was plotted using Wolfram Mathematica 11. The resulting computational model demonstrates the exact three-dimensional boundaries required for the stable confinement of the injected MASER radiation.

In standard free-space electrodynamics, microwave radiation propagates linearly and disperses. However, within the highly refractive, azimuthally flowing fusion plasma of the Tokamak, the MASER beam undergoes continuous momentum exchange. Governed by the strict dimensional equilibrium of the N/m^3 force densities, the electromagnetic wave is guided into a closed, continuous loop.

This toroidal configuration represents a macroscopic **electromagnetic eigenmode**—a stable, resonant standing wave that spans the entire volume of the Tokamak. Functioning analogously to a three-dimensional Whispering Gallery Mode, the geometry ensures that the MASER radiation continuously reflects and propagates along the azimuthal axis without cross-field thermal leakage. Because the calculated force densities at the boundaries are exactly zero ($\Sigma f = 0$), the field configuration is perfectly self-sustaining. The microwave energy is mathematically locked into this toroidal topology, allowing it to maintain the critical central velocity anti-node (maximum heating at the plasma core) while rigorously enforcing the velocity node at the physical boundaries (protecting the reactor walls).

Physical Interpretation of the Equations:

1. **Zero Poloidal Flow** $(e_{v,\theta} = m_{v,\theta} = 0)$**:** The equations mathematically enforce that there is no field dissipation or leakage in the purely poloidal direction. The energy is strictly bounded within the radial (**r**) and azimuthal (φ) planes, preventing turbulent cross-field degradation.
2. **The Toroidal Scale Factor:** The repeating presence of the term $(\cosh r - \cos\theta)$ represents the fundamental Lamé scale factor for toroidal coordinates, proving that these equations are perfectly adapted to the physical geometry of a Tokamak confinement vessel.
3. **Electromagnetic Orthogonality:** The cross-symmetry of the $\mathbf{f_{13}}$ and $\sqrt{K_1 - f_{13}^2}$ terms between the radial and azimuthal components of $\mathbf{e_v}$ and $\mathbf{m_v}$ ensures that the electric and magnetic fields remain strictly orthogonal at all points in space and time. This generates the stable volumetric force density (N/m^3) necessary to exert continuous inward pressure on the plasma, sustaining the central velocity anti-node.
4. The force densities equal exactly zero in every spatial direction $(\Sigma f_r = 0, \Sigma f_\theta = 0, \Sigma f_\phi = 0)$.

7.3 Physical Implications: The Toroidal Electromagnetic Eigenmode

While classical electrodynamics often models electromagnetic wave propagation in a vacuum as strictly linear, the localized toroidal coordinate formulation above mathematically dictates a continuous, closed-loop trajectory. The concept of an electromagnetic wave circulating indefinitely within a toroidal geometry is highly non-intuitive when viewed through the lens of free-space optics, yet it is a well-established phenomenon in advanced wave mechanics and nonlinear plasma physics.

First, within the domain of microwave engineering and macroscopic electrodynamics, this behaviour is analogous to a **Whispering Gallery Mode (WGM)**. In a purely geometric sense, the Tokamak vessel, combined with the ultra-dense, highly refractive flowing plasma, acts as a macroscopic, three-dimensional toroidal waveguide. The electromagnetic wave does not propagate freely; its boundary conditions are strictly enforced by the curved inner geometry of the cavity, allowing the wave to perfectly reflect and circulate continuously without cross-field leakage.

Furthermore, the fusion plasma is not a passive vacuum but a highly nonlinear optical medium. As the intense microwave energy of the MASER propagates through the plasma, it fundamentally alters the local refractive index via ponderomotive forces and thermal expansion. This induces **relativistic self-focusing** (or self-channelling), wherein the electromagnetic wave effectively hollows out its own localized waveguide through the dense medium. Because the entire plasma body is flowing azimuthally (subjected to the continuous Fizeau drag mechanisms established in Chapter 3), this self-generated optical channel is naturally bent into a stable, closed toroidal loop.

From a theoretical standpoint, the mathematical closure of these coupled fields shares a profound lineage with John Archibald Wheeler's concept of the GEON (Gravitational Electromagnetic Entity)—a localized electromagnetic wave self-trapped in a closed orbit. However, whereas Wheeler's GEON relied on intense gravitational curvature to confine the light, the LIFE framework achieves exact topological closure by substituting gravitation with the mathematically equivalent localized acceleration and volumetric force density gradients of the Tokamak plasma.

7.4 Analytical Verification of 3-D Macroscopic Equilibrium

To rigorously validate the stability of this derived topological field configuration, the complete set of hyperbolic and trigonometric equations governing $\mathbf{e_v}$ and $\mathbf{m_v}$ (as depicted in Figure 16) was analytically evaluated using Wolfram Mathematica.

The computational analysis was structured to calculate the net volumetric force density ($\Sigma \mathbf{f}$, strictly evaluated in N/m^3) resulting from the localized interference of the electromagnetic fields across all three spatial dimensions. The computational evaluation unequivocally demonstrates that the resulting force densities equal exactly zero in every spatial direction ($\Sigma f_r = 0$, $\Sigma f_\theta = 0$, $\Sigma f_\phi = 0$).

This zero-force-density result is mathematically profound. It proves that the derived field configuration exists in a state of **perfect dynamic equilibrium**. The outward radiation pressure of the confined electromagnetic wave is flawlessly balanced by the

inward spatial geometry of the toroidal coordinates, and the inherently orthogonal, phase-locked electric and magnetic fields generate no unbalanced turbulent forces. Consequently, this computational verification confirms that the proposed LIFE framework successfully models a stable, non-dissipative, three-dimensional electromagnetic soliton natively adapted to toroidal fusion confinement.

8 The Fundamental Nuclear Plasma-Fusion Stability Equation

In the realm of thermonuclear-heated plasma, a complex interplay of "mechanical-electromagnetic-gravitational interactions" transpires [42]. These interactions manifest between the ionized nuclear plasma, which engenders electromagnetic fields within the plasma itself, and the powerful external field stemming from the heating microwave radiation.

Central to this intricate system is the fundamental boundary condition governing the interactions within the plasma. This condition dictates that at any given moment, in any spatial direction, the total force densities $\bar{f}$ measured in [N/m³] must consistently sum up to zero across the entire volume encompassed within the construction of the Tokamak. This equilibrium is paramount for sustaining stability and harmonious functioning within the Tokamak structure amidst the dynamic interplay of forces.

$$\bar{f} = \rho \left(\frac{\partial \bar{v}}{\partial t} + \bar{v} \cdot \nabla \bar{v} \right) + \nabla p - \nabla \cdot \left(\zeta \left(\nabla \bar{v} + \left(\nabla \bar{v} \right)^T \right) - \frac{2}{3} \zeta \left(\nabla \cdot \bar{v} \right) \bar{\bar{I}} \right) -$$

$$\frac{1}{c^2} \frac{\partial (\bar{E} \times \bar{H})}{\partial t} + \varepsilon_0 \bar{E} (\nabla \cdot \bar{E}) - \varepsilon_0 \bar{E} \times (\nabla \times \bar{E}) +$$

$$\mu_0 \bar{H} (\nabla \cdot \bar{H}) - \mu_0 \bar{H} \times (\nabla \times \bar{H}) + \bar{g} \rho_M = \bar{0} \quad [\mathrm{N/m^3}]$$

$$\varepsilon_0 (\nabla \cdot \bar{E}) = \rho_E \text{ Electric Charge Density } [\mathrm{C/m^3}] \tag{31}$$

in which: $\mu_0 (\nabla \cdot \bar{H}) = \rho_M$ Magnetic Flux Density [Vs/ m³] or [Wb/ m³]

$\gamma_0 (\nabla \cdot \bar{g}) = \rho_{Mass}$ Mass Density [kg/ m³]

Electric Energy Density: $w_E = \frac{1}{2} \varepsilon_0 E^2$

Magnetic Energy Density: $w_M = \frac{1}{2} \mu_0 H^2$

Gravitational Energy Density: $w_G = \frac{1}{2} \gamma_0 g^2$

$\bar{g} \triangleq$ acceleration (gravitational, linear- or orbital acceleration)

The black-coloured terms in equation (42) are derived from well-established principles such as the Navier-Stokes Equation and LIFE Electrodynamics (7). These terms are rooted in conventional scientific frameworks that have been widely accepted and utilized.

Conversely, the red-coloured terms in equation (42) originate from the New Theory, which introduces the concept of "Electro-Magnetic-Accelerated Field" interactions delineating the dynamic interplay between matter, notably the nuclear plasma, and energy represented by electric and magnetic fields. These red terms embody the innovative insights and novel theoretical perspectives brought forth by the New Theory, offering a fresh approach to understanding interactions between matter and energy within the system.

In equation (42) represents: $\overline{E_E}$ the external electric field intensity from the induced microwave radiation and the external induced Electric Fields in the DTT configuration with the three superconducting systems: the Toroidal (TF), the Poloidal (PF) Field and Central Solenoid (CS) Field, $\overline{E_P}$ the internal poloidal electric field intensity generated by the charged particles inside the plasma , $\overline{H_E}$ the external magnetic field intensity from the microwave radiation and the externally induced Magnetic Fields in the DTT configuration with the three superconducting systems: the Toroidal (TF), the Poloidal (PF) Field and Central Solenoid (CS) Field , $\overline{H_P}$ the internal (poloidal) magnetic field intensity generated inside the plasma by the spin of the ions, ζ represents the plasma dynamic viscosity, $\overline{v}$ the velocity, $\overline{g}$ the gravitational-, linear- or orbital- acceleration of the electric- and magnetic fields, p the pressure and $\overline{\overline{I}}$ the identity tensor in the Toroidal Tokamak Reactor.

9 Validation of the LIFE Framework: Reduction to Lorentz and Coulomb Forces in Toroidal Coordinates

According Maxwell's equation, the magnetic part in Equation (6.1) can be reduced, only in "Laminar Plasma Flows" into:

$$-\mu_0 \overline{H_E} \times (\nabla \times \overline{H_P}) = -\mu_0 \overline{H_E} \times \overline{j_P} = -\rho \overline{B_E} \times \bar{v} = \rho \bar{v} \times \overline{B_E} = \frac{1}{V_{Volume}} q \left(\bar{v} \times \overline{B_E}\right) \quad (32)$$

In which $\overline{j_P}$ the electric current density of the laminar flow of electrically charged particle and "q" the electric charge of the particles.

According Gauss's law, the electric part in Equation (6.1) can be reduced, only in "Laminar Plasma Flows" into:

$$\varepsilon_0 \overline{E_E} (\nabla . \overline{E_P}) = \overline{E_E} (\nabla . \overline{D_P}) = \overline{E_E} \rho = \frac{1}{V_{Volume}} q_P \overline{E_E} \quad (33)$$

Substituting (32) and (33) in (7) (only valid in laminar Plasma Flows) results in :

$$\bar{f} = \rho \left(\frac{\partial \bar{v}}{\partial t} + \bar{v} \cdot \nabla \bar{v}\right) + \nabla p - \nabla \cdot \left(\zeta \left(\nabla \bar{v} + (\nabla \bar{v})^T\right) - \frac{2}{3} \zeta (\nabla \cdot \bar{v}) \bar{\bar{I}}\right)$$

$$+ \frac{1}{V_{Volume}} q_P \left(\overline{E_E} + \bar{v} \times \overline{B_E}\right) - \frac{1}{c^2} \frac{\partial (\bar{E} \times \bar{H})}{\partial t} - \varepsilon_0 \bar{E} \times (\nabla \times \bar{E}) + \mu_0 \bar{H} (\nabla . \bar{H}) + \bar{g} \rho_M = \bar{0} \ [N/m^3]$$

in which:

$\varepsilon_0 (\nabla . \bar{E}) = \rho_E$ Electric Charge Density $[C/m^3]$

$\mu_0 (\nabla . \bar{H}) = \rho_M$ Magnetic Flux Density $[Vs/m^3]$ or $[Wb/m^3]$

$\gamma_0 (\nabla . \bar{g}) = \rho_{Mass}$ Mass Density $[kg/m^3]$

Electric Energy Density: $w_E = \frac{1}{2} \varepsilon_0 E^2$

Magnetic Energy Density: $w_M = \frac{1}{2} \mu_0 H^2$

Gravitational Energy Density: $w_G = \frac{1}{2} \gamma_0 g^2$

$\bar{g} \triangleq$ gravitational acceleration (34)

The black coloured terms in equation (45) follow from the Navier Stokes Equation and Classical Electrodynamics. The green coloured terms in equation (45) follow from the LIFE Theoretical Framework describing "Electro-Magnetic-Accelerated

Field" interactions between matter (nuclear plasma) and the MASER energy (electric- and magnetic fields).

This confirms that the unified N/m^3 equilibrium inherently satisfies classical electrodynamics while providing the extended boundary conditions necessary for the resonant cavity discussed in previous chapters.

10 Validation of the LIFE Framework: Reduction to Lorentz and Coulomb Forces in Toroidal Coordinates

Masers, particularly high-power free-electron masers (FEMs), are essential in tokamak nuclear fusion for electron cyclotron resonance heating (ECRH) and current drive to achieve and maintain the necessary 100 million-degree plasma temperatures. They provide high-frequency, high-power microwave radiation (100–300 GHz) to stabilize plasma instabilities and efficiently heat electrons

A characteristic effect of the Nuclear Plasma, confined in a "Tokamak Reactor", are the rotations of the Confined Nuclear Plasma in the Polar Direction and the Angular direction in Toroidal Coordinates [r, θ ,ϕ, α] . In which [θ] represents the angle in the polar direction and [ϕ] represents the angle of rotation in the azimuthal direction. The local radius has been represented by [r] and the radius of the Torus by [α] .

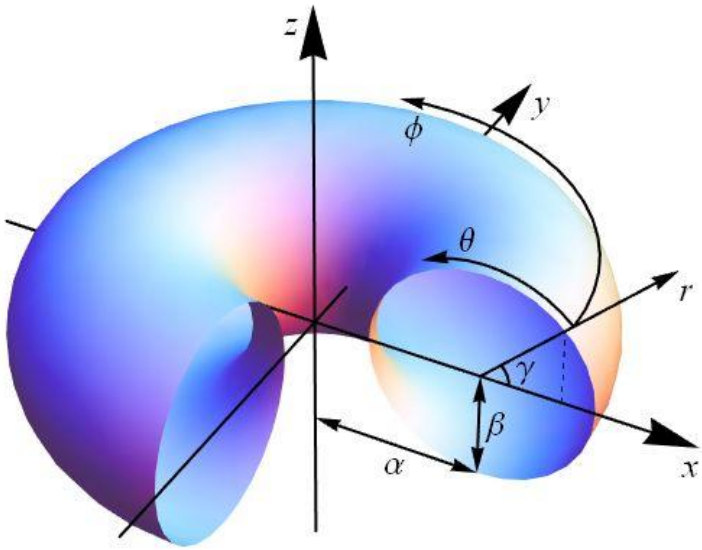

$$(r, \theta, \phi) = \left(\sqrt{\left(\sqrt{x^2 + y^2} - \alpha \right)^2 + z^2} \, , \left(\tan^{-1} \frac{z}{\sqrt{x^2 + y^2} - \alpha} \right) - \gamma, \tan^{-1} \frac{y}{x} \right)$$

$$(x, y, z) = ((\alpha + r\cos(\theta + \gamma))\cos\phi, (\alpha + r\cos(\theta + \gamma))\sin\phi, r\sin(\theta + \gamma))$$

Fig. 13 Representation of Toroidal Coordinates

According Maxwell's equation, the magnetic part in Equation (42) can be reduced, only in "Laminar Plasma Flows" into:

$$\mu_0 \overline{H_E} \times (\nabla \times \overline{H_P}) = \mu_0 \overline{H_E} \times \overline{j_P} = \rho \overline{B_E} \times \bar{v} = -\rho \bar{v} \times \overline{B_E} = - \frac{1}{V_{Volume}} q \left(\bar{v} \times \overline{B_E}\right) \qquad (35)$$

In which $\overline{j_P}$ the electric current density of the laminar flow of electrically charged particle and "q" the electric charge of the particles.

According Gauss's law, the electric part in Equation (42) can be reduced, only in "Laminar Plasma Flows" into:

$$-\varepsilon_0 \overline{E_E} (\nabla . \overline{E_P}) = - \overline{E_E} (\nabla . \overline{D_P}) = - \overline{E_E} \rho = - \frac{1}{V_{Volume}} q_P \overline{E_E} \qquad (36)$$

Substituting (43) and (44) in (42) (only valid in laminar Plasma Flows) results in :

$$\bar{f} = \rho \left(\frac{\partial \bar{v}}{\partial t} + \bar{v} \cdot \nabla \bar{v}\right) + \nabla p - \nabla \cdot \left(\zeta \left(\nabla \bar{v} + (\nabla \bar{v})^T\right) - \frac{2}{3} \zeta (\nabla \cdot \bar{v}) \bar{\bar{I}}\right)$$

$$- \frac{1}{V_{Volume}} q_P \left(\overline{E_E} + \bar{v} \times \overline{B_E}\right) + \frac{1}{c^2} \frac{\partial (\overline{E_E} \times \overline{H_E})}{\partial t} + \frac{1}{c^2} \frac{\partial (\overline{E_P} \times \overline{H_P})}{\partial t} + \varepsilon_0 \overline{E_E} \times (\nabla \times \overline{E_P})$$

$$- \mu_0 \overline{H_E} (\nabla . \overline{H_P}) - \bar{g} \left(\frac{1}{2 c^2} \left(\varepsilon E_E^2 + \mu H_E^2\right)\right) - \gamma_0 \bar{\Gamma} (\nabla . \bar{\Gamma}) + \gamma_0 \bar{\Gamma} \times (\nabla \times \bar{\Gamma}) = \bar{0} \ [N/m^3]$$

$$\varepsilon_0 (\nabla . \bar{E}) = \rho_E \text{ Electric Charge Density } [C/m^3] \qquad (37)$$

in which: $\mu_0 (\nabla . \bar{H}) = \rho_M$ Magnetic Flux Density [Vs/ m^3] or [Wb/ m^3]

$\gamma_0 (\nabla . \bar{g}) = \rho_{Mass}$ Mass Density [kg/ m^3]

Electric Energy Density: $w_E = \frac{1}{2} \varepsilon_0 E^2$

Magnetic Energy Density: $w_M = \frac{1}{2} \mu_0 H^2$

Gravitational Energy Density: $w_G = \frac{1}{2} \gamma_0 g^2$

$\bar{\Gamma} \triangleq$ generalized effective acceleration (gravitational, polar- or azimuthal acceleration)

The black coloured terms in equation (45) follow from the Navier Stokes Equation and Classical Electrodynamics. The green coloured terms in equation (45) follow

from the LIFE Theoretical Framework describing “Electro-Magnetic-Accelerated Field” interactions between matter (nuclear plasma) and the MASER energy (electric- and magnetic fields).

This confirms that the unified N/m^3 equilibrium inherently satisfies classical electrodynamics while providing the extended boundary conditions necessary for the resonant cavity discussed in previous chapters.

11. Conclusions

The interaction between Gravity and Light is effectively described in General Relativity through a 4-dimensional curvature encompassing Space and Time due to the presence of a gravitational field. Light follows a trajectory dictated by this curved 4-dimensional Space-Time geometry.
Contrasting with General Relativity, the new theory introduces a novel concept where mass and inertia within light, represented by photons, exhibit a bi-directional separation. Inertia specifically manifests along the beam's propagation, impacting the speed of light, while mass is oriented perpendicularly, influencing light deflection by gravitational fields. BLACK HOLES, representing Gravitational-Electromagnetic Confinements, serve as fundamental solutions derived from the relativistic quantum mechanical Dirac equation, showcasing significant "Gravitational Intensity Shift" and "Gravitational RedShift" phenomena.

The new theory delves into gravitational fields around BLACK HOLES, investigating the phenomenon of "CURL" within these regions, as well as exploring Gravitational Lensing effects. Gravitational-Electromagnetic Confinements at sub-atomic dimensions characterize physical reality, forming solutions of the Relativistic Quantum Mechanical Dirac Equation, presenting discrete energy levels within spherical confines.

Validating this new theory against General Relativity demands precise experiments measuring Gravity-Light interactions. The distinction in Gravitational RedShift predictions between General Relativity and the New Theory, though minute (smaller than 10^{-16}), necessitates improved observation equipment for validation. Dark Matter's existence, inferred from Gravitational RedShift and Gravitational Intensity Shift effects, elucidates cosmic invisibility implicating billions of light-emitting galaxies beyond the "Gravitational Shielding" radius.

In the domain of nuclear fusion, a new theoretical approach accommodating "mechanical-electromagnetic" interactions in compressible nuclear plasmas espouses stability requirements. Equations (42) and specifically laminar Plasma Flows (45)

signify the 3-dimensional equilibrium between dynamic- and electromagnetic force densities crucial for ensuring the fundamental stability essential for successful nuclear fusion endeavours.

Data Availability

[A] Vegt, W. (2026). 3-D Macroscopic Electromagnetic Equilibrium in Toroidal Coordinates within the LIFE Framework [Mathematica Notebook]. Published on the Wolfram [Community/Demonstrations] site. URL: https://community.wolfram.com/groups/-/m/t/3115543?p_p_auth=8VRRtDct

All Data and Calculations have been published at:

https://quantumlight.science/

References

[1]; GEONs, Physical Review Journals Archive, 97, 511, Issue 2, pages 511-526, Published 15 January 1955, Publisher: American Physical Scociety, DOI: 10.1103/PhysRev.97.511:

[2] Sven Herrmann, Felix Finke, Martin Lülf, Olga (et. Al.) l; Test of the Gravitational Redshift with Galileo Satellites in an Eccentric Orbit ;Phys. Rev. Lett. **121**, 231102 – Published 4 December 2018; Gravitational Redshift Test Using Eccentric Galileo Satellites, DOI: 10.1103/PhysRevLett.121.231102

[3] Vegt, J. W. A Continuous Model of Matter based on AEONs, Physics Essays, Volume 8, Number 2, 1995, DOI: 10.31219/osf.io/ra7ng

[4] Vegt W. Mathematical Solutions for the Propagation of Light in Quantum Light Theory, 2023, Calculations in Mathematica 13.1: https://community.wolfram.com/groups/-/m/t/2576692?p_p_auth=mTldHX3v

[5] Vegt W. Gravitational RedShift between two Atomic Clocks; 2023; Calculations in Mathematica 13.1: https://community.wolfram.com/groups/-/m/t/2622560?p_p_auth=EC8QO0Xz

[6] Propagation of Light within a Gravitational Field in LIFE (Local Interaction Field Equilibrium), Calculation in Mathematica 13.1: https://community.wolfram.com/groups/-/m/t/2576537?p_p_auth=iljE3giH

[7] A. Einstein; On the Influence of Gravitation on the Propagation of Light; Annalen der Physik (ser. 4), **35**, 898–908, http://myweb.rz.uni-augsburg.de/~eckern/adp/history/einstein-papers/1911_35_898-908.pdf

[8] Mahendra Goray, Ramesh Naidu Annavarapu, Rest mass of photon on the surface of matter, Results in Physics 16 (202) 102866, January 2020, DOI: 10.1016/j.rinp.2019.102866
[9] Wim Vegt, The Origin of Gravity, A second order Lorentz Transformation for "Accelerated Electromagnetic Fields", Generating a Gravitational Field and the property of Mass, International Research Journal of Pure and Applied Physics https://www.rroij.com/peer-reviewed/the-origin-of-gravity-91966.html
[10] Vegt W., The 4-Dimensional Dirac Equation in Relativistic Field Theory, European Journal of Applied Sciences, Vol 9, No. 1, pp 35 – 93,2021
[11] John G. Williamson; A new linear theory of light and matter; 2019; J. Phys.: Conf. Ser. 1251 012050 DOI https://doi.org/10.1088/1742-6596/1251/1/012050
[11] BLACK HOLEs with Discrete Spherical Energy Levels: https://community.wolfram.com/groups/-/m/t/2896941?p_p_auth=D7ZKuo3k
[12] Vegt W. Time and Radius dependent GEONs with discrete Energy Levels https://community.wolfram.com/groups/-/m/t/2900869?p_p_auth=yxR9nZu6
[13] Time and Angular Regions dependent GEONs with discrete energy levels. https://community.wolfram.com/groups/-/m/t/2901457?p_p_auth=H4jjDHmQ
[14] Time and Azimuthal Regions dependent GEONs with discrete energy levels https://community.wolfram.com/groups/-/m/t/2902170?p_p_auth=yt0q5nEh
[15] Time, Polar Angular and Azimuthal Angular Regions dependent GEONs with discrete energy levels https://community.wolfram.com/groups/-/m/t/2902642?p_p_auth=sW2mvv9L
[16] D. W. Sciama; The Physical Structure of General Relativity; Rev. Mod. Phys. 36, 463 – Published 1 January 1964; Erratum Rev. Mod. Phys. 36, 1103 (1964)
[19] Adrian del Rio, Jose Navarro-Salas, and Francisco Torrenti; Renormalized stress-energy tensor for spin -1/2 fields in expanding universes; Phys. Rev. D 90, 084017 – Published 13 October 2014
[20] Stergios Pellis; Unity Formulas for the Coupling Constants and the Dimensionless Physical Constants; Journal of High Energy Physics Gravitation and Cosmology; DOI: 10.4236/jhepgc.2023.91021
[21] Bloch, Yakov and Joshua Foo. "How the result of a measurement of a photon's mass can turn out to be 100." (2023). Corpus ID: 258426255
[22] Andrés Arámburo García, Kyrylo Bondarenko, Sylvia Ploeckinger, Josef Pradler and Anastasia Sokolenko; Effective photon mass and (dark) photon conversion in the inhomogeneous Universe; Journal of Cosmology and Astroparticle Physics, Volume 2020, October 2020
[23] Alexander M Gabovich and Nadezhda A Gabovich; How to explain the non-zero mass of electromagnetic radiation consisting of zero-mass photons; European Journal of Physics; 2007; 28 649; DOI 10.1088/0143-0807/28/4/004
[24] Liang-Cheng Tu, Jun Luo and George T Gillies; The mass of the photon; Reports on Progress in Physics, Volume 68, Number 1; DOI 10.1088/0034-4885/68/1/R02

[25] Doyon, B. Conformal Loop Ensembles and the Stress–Energy Tensor. Lett Math Phys 103, 233–284 (2013). https://doi.org/10.1007/s11005-012-0594-1
[26] T. P. Hack and V. Moretti; On the stress–energy tensor of quantum fields in curved spacetimes—comparison of different regularization schemes and symmetry of the Hadamard/Seeley–DeWitt coefficients; 2012 J. Phys. A: Math. Theor. 45 374019; DOI: 10.1088/1751-8113/45/37/374019
[27] Adam Levi; Renormalized stress-energy tensor for stationary black holes; Phys. Rev. D 95, 025007 – Published 10 January 2017; https://doi.org/10.1103/PhysRevD.95.025007
[28] Gobbi, Julio; Luminiferous Æther: General Science Journal; December 10, 2018 γ_0 = Gravitational permeability of vacuum [kg s2 m-3]
[29] Xing-Hao Ye, Qiang Lin; Gravitational Lensing Analyzed by Graded Refractive Index of Vacuum; Journal of Optics A: Pure and Applied Optics; 1 May 2008; DOI 10.1088/1464-4258/10/7/075001
[31] P. Delva, N. Puchades, E. Schönemann, F. Dilssner, C. Courde (et. all); Gravitational Redshift Test Using Eccentric Galileo Satellites; Phys. Rev. Lett. 121, 231101 – Published 4 December 2018; DOI: 10.1103/PhysRevLett.121.231101
[32] Oppenheim, Jonathan, A Postquantum Theory of Classical Gravity, Phys. Rev. X, Vol. 13, December 2023; DOI: https://doi.org/10.1103/PhysRevX.13.041040
https://www.rroij.com/peer-reviewed/the-origin-of-gravity-91966.html
[35] Wim Vegt; A Perfect Equilibrium inside a Black Hole; Wolfram Community: https://community.wolfram.com/groups/-/m/t/3087823?p_p_auth=dpH7iBMg
[36] Albert Einstein, "Elementare Uberlegungen zur Interpretation der Grundlagen der Quanten-Mechanik", Translated into English, 2011, DOI: https://doi.org/10.48550/arXiv.1107.3701
[37] Nikko John Leo S. Lobos, Reggie C. Pantig; Generalized Extended Uncertainty Principle Black Holes: Shadow and lensing in the macro- and microscopic realms; Physics 2022, 4(4), 1318-1330; https://doi.org/10.3390/physics4040084
[38] Zihua Weng, Influence of velocity curl on conservation laws, October 2008, https://doi.org/10.48550/arXiv.0810.0065
[39] Peter Vadasz, Rendering the Navier–Stokes Equations for a Compressible Fluid into the Schrödinger Equation for Quantum Mechanics, MDPI-Fluids, May 2016, https://doi.org/10.3390/fluids1020018
[40] Young-Sam Kwon, Asymptotic limit for rotational quantum compressible Navier–Stokes equations with multiple scales, Journal of Mathematical Analysis and Applications, Volume 464, Issue 2, 15 August 2018, Pages 1408-1424, https://doi.org/10.1016/j.jmaa.2018.04.073
[41] Senjo Shimizu and Hidenobu Tsuritani, On a Navier–Stokes–Ohm problem from plasma physics in multi connected domains, Partial Differential Equations and Applications (2021) 2:75, https://doi.org/10.1007/s42985-021-00122-7

[42] Jean-Luc Cambier and David A. Micheletti, Theoretical Analysis of the Electron Spiral Toroid Concept , NASA/CR-2000-210654, https://ntrs.nasa.gov/api/citations/20010021117/downloads/20010021117.pdf
[43] Soraya Field Fiorio, Isaac Newton: Magician, https://parabola.org/2020/11/01/isaac-newton-magician/
[44] J.D. Sethian, M. Friedman e.a.; Fusion energy with lasers, direct drive targets, and dry wall chambers; Nuclear Fusion, Volume 43, Number 12; **DOI** 10.1088/0029-5515/43/12/015
[45] Degrave, J., Felici, F., Buchli, J. et al. Magnetic control of tokamak plasmas through deep reinforcement learning. Nature 602, 414–419 (2022). https://doi.org/10.1038/s41586-021-04301-9